AD-A161 953 TRANSONIC UNSTEADY AERODYNAMICS AND ITS AEROELASTIC APPLICATIONS HELD AT..(U) ADVISORY GROUP FOR AEROSPACE RESEARCH AND DEVELOPMENT NEUILLY.. JUN 85 1/1

UNCLASSIFIED AGARD-CP-374-ADD-1 F/G 20/4 NL

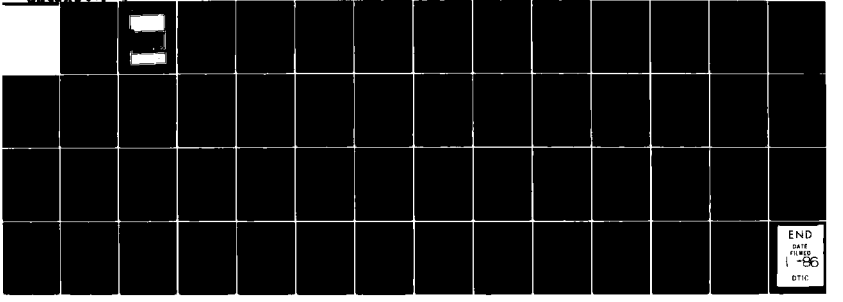

END
DATE FILMED
1-86
DTIC

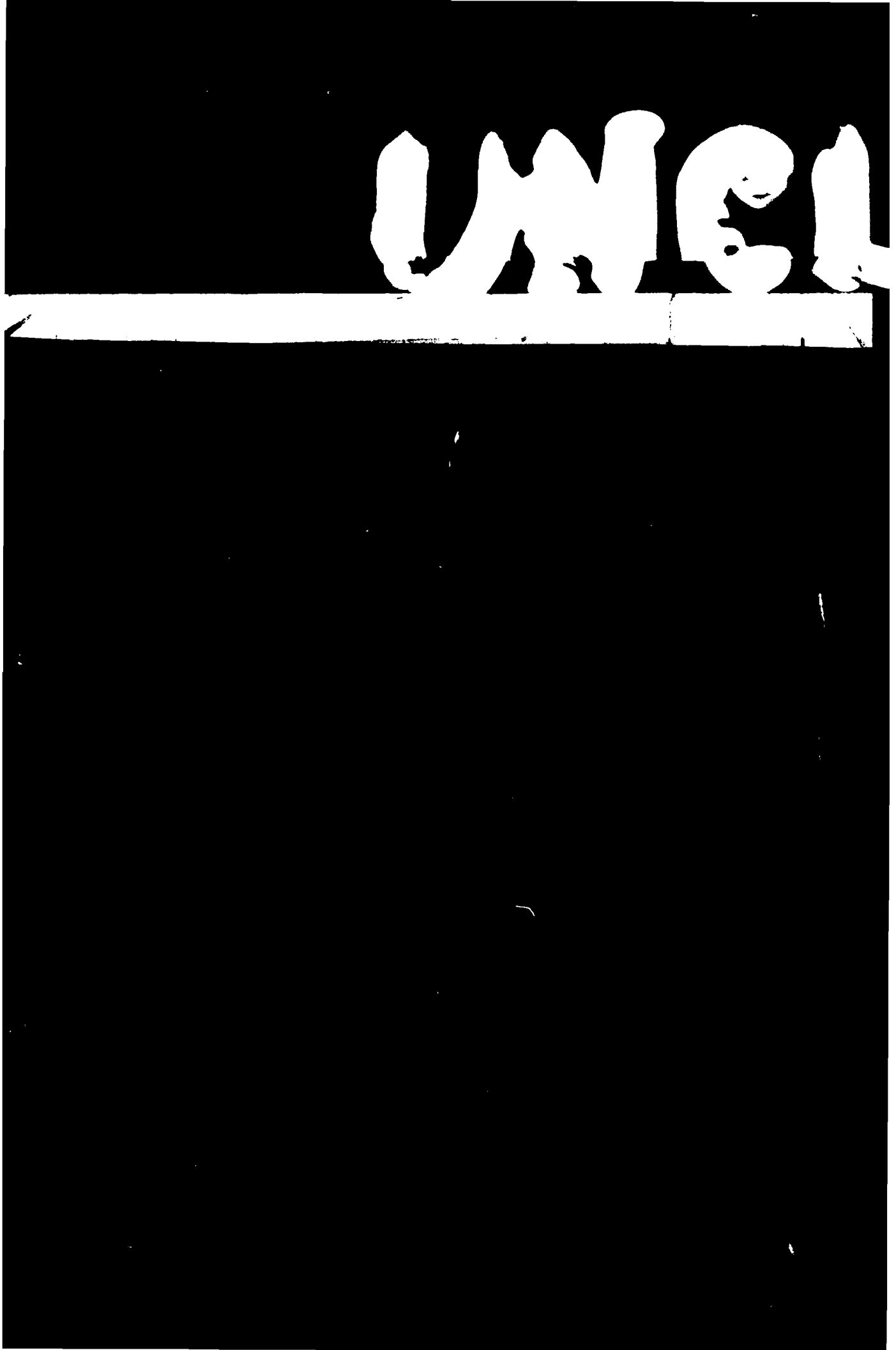

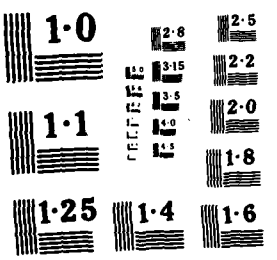

AGARD-CP-374 Addendum I

AGARD

ADVISORY GROUP FOR AEROSPACE RESEARCH & DEVELOPMENT

7 RUE ANCELLE 92200 NEUILLY SUR SEINE FRANCE

AGARD CONFERENCE PROCEEDINGS No.374

Transonic Unsteady Aerodynamics and its Aeroelastic Applications

Addendum 1

NORTH ATLANTIC TREATY ORGANIZATION

AGARD-CP-374
Addendum 1

NORTH ATLANTIC TREATY ORGANIZATION

ADVISORY GROUP FOR AEROSPACE RESEARCH AND DEVELOPMENT

(ORGANISATION DU TRAITE DE L'ATLANTIQUE NORD)

AGARD Conference Proceedings No.374

Addendum 1

TRANSONIC UNSTEADY AERODYNAMICS AND ITS AEROELASTIC APPLICATIONS

A review of the papers presented at the 59th Meeting of the Structures and Materials Panel in Toulouse, France, 2—7 September 1984, together with a record of the Round Table Discussion.

THE MISSION OF AGARD

The mission of AGARD is to bring together the leading personalities of the NATO nations in the fields of science and technology relating to aerospace for the following purposes:

- Exchanging of scientific and technical information;
- Continuously stimulating advances in the aerospace sciences relevant to strengthening the common defence posture;
- Improving the co-operation among member nations in aerospace research and development;
- Providing scientific and technical advice and assistance to the North Atlantic Military Committee in the field of aerospace research and development;
- Rendering scientific and technical assistance, as requested, to other NATO bodies and to member nations in connection with research and development problems in the aerospace field;
- Providing assistance to member nations for the purpose of increasing their scientific and technical potential;
- Recommending effective ways for the member nations to use their research and development capabilities for the common benefit of the NATO community.

The highest authority within AGARD is the National Delegates Board consisting of officially appointed senior representatives from each member nation. The mission of AGARD is carried out through the Panels which are composed of experts appointed by the National Delegates, the Consultant and Exchange Programme and the Aerospace Applications Studies Programme. The results of AGARD work are reported to the member nations and the NATO Authorities through the AGARD series of publications of which this is one.

Participation in AGARD activities is by invitation only and is normally limited to citizens of the NATO nations.

Published June 1985

ISBN 92-835-1501-3

Printed by Specialised Printing Services Limited
40 Chigwell Lane, Loughton, Essex IG10 3TZ

PREFACE

The Fall 1984 Structures and Materials Panel held a Specialists' Meeting on Transonic Unsteady Aerodynamics and its Aeroelastic Applications. This Meeting was the culmination of the Panel's effort in asking aeroelasticians in the various NATO countries to evaluate their methods of calculation against the AGARD—SMP Standard Aeroelastic Configurations. The papers for this Meeting were published in the main volume of the Conference Proceedings. This addendum contains a review of these papers and the discussions thereon.

J.J.OLSEN
Chairman, Sub-Committee
on Aeroelasticity

REVIEW OF SMP 1984 SYMPOSIUM ON "TRANSONIC UNSTEADY AERODYNAMICS AND ITS AEROELASTIC APPLICATIONS"

Walter J. Mykytow
14 Old Stone Way (Unit 9)
Weymouth, Massachusetts 02189
U.S.A.

SUMMARY

The 59th meeting of the AGARD Structures and Materials Panel was held on 3-7 September 1984, in Toulouse, France. It included a specialists' conference to discuss the latest methods of predicting transonic unsteady airloads for oscillating surfaces and flutter. Also considered were aeroelastic applications, many of which were made to standard configurations selected for the SMP cooperative program. This paper summarizes the 16 papers and the round table discussion in some detail for coordinations with AGARD's Fluid Dynamics Panel and Fluid Mechanics Panel.

INTRODUCTION

This specialists' meeting in Toulouse, France, in September 1984, could be considered the third of a series on transonic unsteady aerodynamics and aeroelastic applications.

The first AGARD SMP meeting was held in Lisbon, Portugal, in April 1977, and was entitled "Unsteady Airloads in Separated and Transonic Flow" (AGARD CP-226). Some of the subject matter concerned:

1. Reduced damping in bending during model tests of swept back wings.
2. Wing torsional buzz in flight and in model tests.
3. Reduction of flutter speeds due to leading edge vortex.
4. History of various aircraft flutter problems.
5. Wind tunnel wall porosity effects on flutter.
6. Unsteady pressure measurements on NLR-7301 airfoil.
7. Euler-viscous ramp calculations for NACA 64A-006 oscillating airfoil.
8. LTRAN applications to predict disappearing shocks, wall effects, coupled aero-structural response in pitch, and indicial aerodynamic parameters.
9. Euler calculations for pitching airfoil with boundary conditions on exact airfoil.
10. Garner's semiempirical method for computing transonic unsteady airloads.
11. Time-linearized relaxation methods for a rectangular wing.
12. Proper treatment of shock movements and jump conditions.
13. Numerical instabilities in the relaxation process.

The second AGARD SMP meeting was held in Aix-en-Provence, France, in September 1980, and was entitled "Boundary Layer Effects on Unsteady Airloads" (AGARD CP-296). Topics at this meeting included:

1. Demarcation of linear and nonlinear zones by a shock displacement criterion.
2. Application of TSP-viscous ramp method to NLR-7301 airfoil.
3. Levels of closure in unsteady turbulent flow. Transport equations and the inverse method
4. Unsteady Kutta condition, boundary layer displacement effects, gap flow for controls, and vortex effects.
5. Deduction of boundary layer effects versus frequency by comparison of experimental data and inviscid calculations. Weak coupling viscous effects for oscillating flap. Reversed shock movement in separated flow as flap angle increased. Aerodynamic resonance for NLR-7301 airfoil.
6. Application of the strong coupling method and TSP to oscillating flap in non-separated flow.
7. Application of Garner's semiempirical method to flutter model test data with success.
8. Application of Navier-Stokes method to airfoil with changing incidence at subsonic speeds.
9. Test data for airfoils with separated flow and Reynolds number effects. Anomalous behavior of unsteady airloads with frequency for separated flow.
10. The poor state of art for predicting unsteady airloads for control surfaces.
11. Flow instabilities over (nonmoving, rigid) thick, biconvex airfoils. Self-induced flow oscillations.
12. Boundary layers and cyclic pressure variations at subsonic speeds in a low speed tunnel.

The transonic region is the most critical one for aircraft static and dynamic aeroelastic problems. Reliable methods to predict unsteady transonic airloads had been lacking. However in 1977 it appeared practical to numerically simulate transonic unsteady physical phenomena for industrial applications. The AGARD Structures and Materials Panel therefore initiated a Working Group and a cooperative program. Standard configurations were selected for calculations and comparisons of computed transonic unsteady airloads. Seven conditions were selected for airfoils and five for 3-D wings (AGARD AR-156; AGARD AR-167; AGARD R-673; and AGARD R-702). Separated flow cases were not selected.

GENERAL COMMENTS ON SMP MEETING

The above background information then serves as a basis to judge the recent remarkable progress and the very noticeable success of AGARD SMP's cooperative program.

Sixteen papers were presented at this conference in Toulouse. Two of these concerned speed and memory capabilities of future computers. Milestones in unsteady CFD are mentioned together with limiting features and the possibilities for overcoming them. Dramatic time and cost reductions for future computations are forecast. With NASA's Numerical Aerodynamic Simulation Program, a 15-minute run before 1988 is quoted as possible for the application of the unsteady full potential method to a 3-D wing. Another optimistic hope, based on overcoming serious limitations, was that a reliable simulation of viscous transonic unsteady flow around a fighter might be possible in a decade.

Methods presented for predicting transonic unsteady airloads included time-linearized transonic perturbation, TSP, full potential and Euler methods for 2-D airfoils and 3-D wings. One report concerned applications of the 2-D Navier-Stokes method using an eddy-viscosity model based on simple steady flow experiments. Other modeling of viscous effects included matching of flow conditions by angle and Mach number changes, airfoil modifications, the viscous ramp, and weak or strong coupling of inner viscid flow and outer inviscid TSP flow. Several calculations were made for transonic separated flow on airfoils with some success. Two papers dealt with applications to supersonic flow fields.

One paper presented results of calculations for 2-D pitch-plunge flutter simulating the effects of a swept wing. The flutter calculations were made using TSP, linearized TSP, Euler, and corrected and uncorrected doublet lattice methods with noticeably different results. One other paper also presented 2-D flutter calculations. Five 3-D flutter calculations were also reported, several with rather good agreement with test data, indicating the initial transition of transonic unsteady aerodynamics from a research-scientific status towards industrial applications. One of the papers showed a second transonic flutter dip from model tests in separated flow. Inviscid 3-D methods were extended to highly swept wings of low aspect ratio.

Most of the calculated-test correlations are made for airfoils, but several applications were made to wings and control surfaces.

Some new test data were presented for airfoils in pitch or for flap rotation. More test data for plunge are now available. One paper presented data for an oscillating split-flap spoiler. Approximate calculations showed promise for rough prediction of subsonic unsteady spoiler loads.

Wall effect contamination of both quasisteady and low frequency test data was frequently mentioned. Also questioned several times were model surface conditions, low Reynolds number testing, and large model-wind tunnel dimensional ratios which caused interference. Reliable methods to predict wall effects are not available. Brief comments were made about the difficulty of such predictions and on tunnel resonances, unsteady wake effects, diffuser wall effects, corners, etc.

Higher nonlinear effects and larger, higher order harmonics were noticed in unsteady test data near oscillating strong shocks and separated flow. Their effects on flutter characteristics were not completely evaluated although previous investigations on airfoils under less severe conditions indicated that such higher order harmonics could be ignored in integrated airloads. Some evaluations of strongly nonlinear unsteady aerodynamic effects were deemed advisable to determine whether linear procedures in flutter analyses were still applicable.

Most numerical-test comparisons were made on the basis of unsteady pressure distributions. This data and other basic data are still required. More comparisons are needed on integrated sectional lift and moment coefficients, and are forthcoming from SMP's cooperative program. Comparisons of generalized aerodynamic forces used in typical flutter analyses were deemed highly desirable.

Information was presented for both conventional and supercritical airfoils. A few comments questioned the applicability of supercritical airfoils to fighter designs and to aircraft employing active controls and aeroelastic tailoring. High angle of attack information is needed for maneuvering fighters while aeroelastic deformations would be important boundary conditions for transports.

Two papers considered high angles. One treated ramping angular changes at constant rate. The other treated prediction of unsteady airloads for large pitch amplitudes.

The methods presented varied significantly in numerical complexity, computer time required, and cost. Some of the simpler methods could have runs of several minutes on modern computers. The more complex methods require hours per run.

Methods likely to be used in the future are difficult to predict. No doubt they will be the simpler and lower cost procedures which will develop in an evolutionary manner; but it was agreed that their acceptances must be validated and justified by comparisons with results from more complex methods and test data.

The selection of SMP standard flutter cases, preferably cases where reliable flutter model data existed, was recommended several times. The application to industrial type flutter problems would include calculation of generalized forces on the basis of given vibration modes and calculations of amplitude ratios and phases at the critical flutter point as well as dynamic pressure and flutter frequency.

There is an urgent need to develop low cost and quick turn around methods for preliminary design and first engineering stages to assure production of efficient aircraft with minimum weight and performance penalties from the start.

This meeting did describe the encouraging progress in predicting transonic unsteady aerodynamic effects such as shock location, movement, strength, and phase. Good qualitative agreement is achieved and trends compare quite reasonably with test data. In many cases, quantitative agreements between tests and calculations are good. Doublet lattice and kernel function methods neglect fundamental transonic effects and produce unconservative flutter speed predictions unless major modifications are made to key parameters. Other predicted data from these linear theories, such as flutter frequency, amplitude ratio and phase, are grossly incorrect frequently. Thus, the new transonic unsteady CFD methods will certainly be applied industrially in the near future.

PAPERS PRESENTED

A semidetailed summary of each paper has been prepared primarily for the appreciation of the new major contributions by the practicing flutter engineer. This summary is then followed by a description of the round table discussion, and finally by general conclusions and recommendations. Complete versions of the papers are given in AGARD SMP CP-374, "Transonic Unsteady Aerodynamics and Its Aeroelastic Applications."[1]

1. V. L. PETERSON: "Trends in Computational Capabilities for Fluid Dynamics"

Milestone developments in CFD, computer capability, cost trends, and future performance requirements were discussed for both inviscid and viscous steady and unsteady flows. The development for unsteady flows and for elastic surfaces has lagged since nonsteady calculations require larger computers and more time-consuming calculations. Real time must be simulated, the technology is more difficult, and fewer scientists are versed both in CFD and structural dynamics. Thus, the total level of effort is lower, and there is lesser availability of user-oriented codes.

The author discussed progress versus time in levels of Navier-Stokes equation approximation. Linearized inviscid level I is mature for both steady and unsteady flows. Nonlinear inviscid level II has advanced, but aeroelastic applications are required. Reynolds-averaged Navier-Stokes level III is costly, and aeroelastic investigations are rare. Large eddy level IV and exact full Navier-Stokes level V are in the early research stages.

Milestones mentioned for inviscid unsteady transonic flow range from small perturbation methods for 2-D airfoils in 1975 to full potential unsteady methods for wings in 1981. Unsteady viscous flow applications were made to airfoil buffet, cavity aeroacoustics, turbulent flow plunge-pitch flutter, and aileron buzz from 1977-1979.

Relative computer costs have dropped markedly due to the rapid computer speed progress (millions of floating point operations per second) and the much lesser growth of rental costs (Figure 1-1). Furthermore, memory has grown 3 to 4 orders of magnitude in 20 years with 500 million words of memory expected about 1990. The improvement in relative costs is about two orders of magnitude in 15 years. With better algorithms, the compounded improvement in relative costs might be 1:100,000.

The authors mentioned that the operations per grid point are 50 times greater for unsteady calculations since 3 cycles of oscillation are generally used and since a factor of 15 is required to simulate time. The factor of 50 might be reduced to 5 with improved algorithms.

An advanced computational facility, NASA's Numerical Aerodynamic Simulation Program, has been proposed and would be available to the U.S. scientific and industrial aerospace community like wind tunnels. Estimates indicate about one minute of computer time would be needed to calculate unsteady viscous flows about 2-D airfoils. Figure 1-2 shows similar estimates for oscillating wings using 1984 algorithms. Simple wing-body combinations are a little more difficult.

The days to weeks of computer time for viscous calculations (Figure 1-2) suggest that near future unsteady aerodynamic and flutter calculations will be limited to nonviscous flows except for special cases or to simpler semiempirical approximations of the viscous effects.

NASA's experience has shown that computer time should be limited to 10 minutes per case if industry is expected to apply these methods in the design environment. Figure 1-3 shows memory-speed requirements for 15-minute computer runs. Unsteady calculations using the full potential method for wings should soon be possible, but unsteady, viscous, 3-D calculations by Reynolds-averaged forms will not be practical for some time to come.

Estimates were made for the time to compute a transonic flutter boundary using 5 Mach numbers, 4 reduced frequencies and 4 modes. An estimate of 37 hours was given using today's computers and inviscid methods. Very practical times of 1 to 2 hours might be achievable by 1988.

The authors emphasized the complementary aspects of combined computational and experimental investigations. Also emphasized was the capability of numerical investigations to provide salient data when experimental facilities were limited or lacking. The Jupiter probe studies were cited as an example.

2. H. TRIEBSTEIN AND R. VOSS: "Transonic Pressure Distributions on a Two-Dimensional NACA 0012 and Supercritical MBB-A3 Profile Oscillating in Heave and Pitch"

These experimental investigations concern effects of reduced frequency, Mach number, oscillation amplitude, angle of attack, separation, and Reynolds number. This paper deals mainly with results for the MBB-A3 airfoil. Results for the NACA 0012 airfoil were given at the September 1984 ICAS meeting.

All four walls of the wind tunnel are perforated. Solid disks were used at the sides of the model. The distance of the model was 1.7 chords from the upper (lower) wall. The design point is M = 0.765 at 1.5 degrees. No transition strips were used. A lambda shock results due to the laminar flow at lower wind tunnel Reynolds numbers.

Figure 2-1 shows the effects of Mach number for pitch oscillations. Typical subsonic trends result for M = 0.5. At M = 0.78, a strong shock peak occurs in the upper side pressure distribution. The real part changes sign due to separation near the trailing edge. The imaginary part changes sign at the shock. Heave oscillation tests show similar results but with imaginary part exchanged with real part relative to pitch. Leading edge (small bubble) flow separation is noticed for heave test data.

Unsteady real-part pressure peaks for pitch (M = 0.78; angle = 0.15 degrees) increase with increasing frequency. This trend is opposite to that expected from theory. The cause is suspected to be the influence of tunnel walls. For heave motions, elastic behavior of the model contaminated results for higher frequencies.

Larger pitch amplitudes decreased the height and increased the width of the unsteady pressure peaks near the shock. Higher harmonics are present near the shock due to the nonlinearity of shock movements and in separation areas. The higher harmonics disappear if the flow reattaches. Nonlinear effects are less evident with chordwise integrations of pressures.

Calculations were performed, for cases where flow was attached and shock strength moderate, by both the LTRAN 2 time integration method and the Geissler-Voss doublet-source, field panel, integral method for the time-linearized small perturbation equation.

The authors stress the need to first have a good prediction of the steady pressure distribution by varying both Mach number and angle to obtain good agreement on the shock position (or of the sonic line) and the supersonic plateau.

For the MBB-A3 airfoil in pitch at a subsonic Mach number of 0.7, agreement between unsteady test and theoretical data was good for the real part, but the zero crossing point for the imaginary part for theory was too far aft. The authors suspect wall interference effects rather than viscous effects.

For higher Mach numbers, the unsteady loading forward of the shock increases with increasing reduced frequency. Figure 2-2 shows results for the design condition at a higher reduced frequency. Notice the higher loading for test results forward of the shock. Wall interference effects may be responsible for this trend which is opposite to that from theory. The large shift towards positive imaginary peaks near the shock might be indicative of separation as shown by other tests and Navier-Stokes calculations. However, yet other data do not substantiate this. Thus, conclusions are not firm.

Results from the two theories differ in shock location and strength, and also in the Mach number and in the regional influence of the supersonic zone.

Agreement between theory and experiment for heave oscillations at design point conditions was not good due to wall effects, low heave loads, and model elasticity.

Pressure calculations for the MBB-A3 airfoil by the time-linearized field panel method for various frequencies at the design condition show chordwise waviness increasing with frequency due to the increasing wave number of the receding waves. Better damping of these upstream waves might result from the use of nonlinear codes and improved grid spacing. The integrated aerodynamic parameters shown in Figure 2-3 do not show these undulations. The values at higher reduced frequencies approach those of linear (flat-plate) theory.

Some Schlieren motion pictures were shown for the NACA 0012 airfoil in separated flow. For a nonmoving airfoil at 5 degrees and low Reynolds number, a lambda shock with separation occurs. A distinct low frequency flow oscillation is seen near the leading edge. Later

pictures show that the separation and lambda shock remain throughout the cycle of the oscillating airfoil. For 2 degrees, there is no lambda shock for the steady airfoil, but it appears at the higher angles when the model oscillates in pitch. The flow reattaches at lower angles. A phase lag of the shock relative to airfoil position is noticed.

This paper provided important new information and dramatically emphasized the effects of wind tunnel walls, separation and viscosity, and model elasticities. Future tests will include transition strips and different wall conditions.

3. W. J. CHYU AND S. S. DAVIS: "Numerical Studies of Unsteady Transonic Flow Over an Oscillating Airfoil"

Unsteady transonic pressures are computed using the 2-D Navier-Stokes equation and a time-varying grid for an oscillating airfoil. A two-layer, Cebeci eddy-viscosity model, where mixing length scale is based on local vorticity, is used for turbulent flows.

Thin layer Navier-Stokes calculations are made for the NACA 64A010 airfoil at small incidences where weak shock-boundary layer interactions occur. The M = 0.8 calculations show reasonably good agreement with experimental instantaneous chordwise pressures for small pitch oscillations over the entire cycle. Negative pressures in front of the shock are overpredicted and wall effects are suspected. Nonlinear time histories of local pressures are well predicted by both thin layer and full Navier-Stokes codes, and almost as well by the Euler method. The chordwise shock location and its 7% motion are better predicted by the thin layer viscous code. Shock data for the full Navier-Stokes code were not shown. Viscous effects are small.

Figure 3-1 shows the first harmonic components of the pressure coefficients. Predictions are good except near the shock. Viscous calculations are better. Imaginary parts grow with increasing frequency and absolute values decrease with frequency in a consistent manner. This is in agreement with theory.

Calculations for pitch oscillations of the NACA 64A010 were also made about a higher mean angle (4 degrees) where strong shock-boundary layer interactions were present for most angles in the cycle. At the highest instantaneous angles (5 degrees) experimental data show slow pressure recovery aft of the shock and separation. As the instantaneous angle decreases to approximately 3 degrees and then up to 3.13 degrees, in an increasing manner, the aft pressure recovery is fast and the flow becomes attached.

While inviscid theory predicts the supersonic plateau reasonably well, the predicted shock is too far aft. Both full and thin layer Navier-Stokes methods show similar results and predict the chordwise instantaneous pressure distribution, shock location and shock (13% chord) travel reasonably well. Predicted suction levels in the plateau ahead of the shock are too high. The N. S. method predicted aft-pressure recoveries fairly well, but the transition angle between slow to fast recoveries (separated versus attached flow) is not well predicted. However, viscous calculations predicted an upstream (reversed) movement of the shock position with increasing angle as has been observed in experiments with separation.

Figure 3-2 shows the comparisons of the first harmonic components of the NACA 64A010 chordwise pressure distributions for a 4-degree mean angle. There are large and complex variations with frequency. The real (in-phase) peaks near the shock change sign with frequency. Real values near the trailing edge are high compared to the low angle, nonseparated flow case of Figure 3-1. Imaginary components also show high values near the trailing edge. Viscous calculations show that the complex trends are predicted qualitatively quite well even though quantitative agreement is not good near the peaks.

The blunt leading edge, 16.5% thick, supercritical NLR 7301 airfoil near the design condition (M = 0.75; angle = 0.37 degree) was the third case considered. Full Navier Stokes calculations were made for instantaneous chordwise pressures for airfoil pitch. Agreement was reasonably good between theory and experiment except near the compression. The test data showed a waviness ahead of the shock due to sensitivity of unsteady responses to the flow field. Figure 3-3 shows experimental and full Navier-Stokes calculations. The mean pressure shows a rapid compression but no shock, fast pressure recovery, and very little separation. The compression results in large real and imaginary first harmonic peaks. The imaginary component at low frequency is relatively large contrary to the result for the conventional airfoil at low angles. Overall, trends are qualitatively predicted. Phases along the chord between real and imaginary parts are reasonably well predicted. Tunnel walls, nonuniform free stream conditions, turbulence levels and airfoil shape tolerances are cited as possible reasons for differences. The tests and calculations show that the unsteady results for this blunt-thick supercritical airfoil are noticeably different than those for conventional airfoils and are sensitive to transonic flow conditions.

The authors conclude that thin layer and full Navier-Stokes methods gave similar results except near shocks and neither gave consistently better agreement. An improved turbulence model is required when viscous effects dominate.

4. R. G. DEN BOER AND R. HOUWINK: "Analysis of Transonic Aerodynamic Characteristics for a Supercritical Airfoil Oscillating in Heave, Pitch and with Oscillating Flap"

Unsteady pressure measurements were made covering a wide range of conditions for an oscillating, 12%-thick, supercritical airfoil. Test angles of attack were corrected for wall effects for the steady case. Wall effects were expected for unsteady tests, possibly giving a positive shift to lift phase angle and decreased lift at low frequency. Lesser effects should occur at higher frequencies.

Test data at the design point angle show increasing unsteady pressures at the trailing edge for the pitching airfoil and an unsteady boundary layer effect as Mach number increases.

Other tests for plunge or flap oscillations show pressure distributions as generally expected.

The effect of angle of attack on pitch oscillations is shown in Figure 4-1. Larger unsteady airloads result for the supercritical airfoil as design point conditions are approached (M = 0.75; angle = 0.75 degrees). Unsteady airload peaks become sharper near the strong shock for an angle of 1.5 degrees. Flow is attached. Finally, for 3.0 degrees, both the real and imaginary parts enlarge. High unsteady pressures are noticed near the trailing edge indicating large boundary layer variations. Flow is separated for the steady 3-degree case and for small changes about this position. The shock moves forward with increasing angle in the separated flow.

For 3 degrees, the peak unsteady pressure modulus increases with increasing frequency up to a reduced frequency of 0.25. (It decreases with increasing frequency for lower angles in unseparated flow.) The phase angle across the chord shows a completely different behavior. Pressures downstream of the shock and at the trailing edge also increase up to a reduced frequency of 0.25. The authors suggest an aerodynamic resonant phenomenon.

The following explanation was offered for one oscillation cycle. As the angle starts from 3 degrees, the flow is essentially attached; but with increasing instantaneous angle, the flow separates while the shock moves forward. The shock strength reaches a maximum three-eighths through the cycle, and the shock is most forward half-way through the cycle when the perturbation angle (about 3 degrees) has reached zero. Negative perturbation angles (about 3 degrees) follow next. The shock moves back with decreasing angle and separation decreases further. The cycle then repeats.

Figures 4-2 and 4-3 show the unsteady lifts and moments for this separated flow. These coefficients are much larger at M = 0.75 than for the attached flow. Other data show an influence of oscillation amplitude on real parts. Corresponding phase angles for attached and separated flow are different. All of the above differences have significant effects on flutter behavior.

The aerodynamic resonance at a reduced frequency of 0.25 is confirmed by a circle diagram plot of imaginary lift component versus real component at various frequencies. Power spectral analyses for lift fluctuations without airfoil motion show that an unsteady flow phenomenon is present. Minimum damping for this phenomenon occurs for angles where the shock motion reverses and when the reduced frequency is near 0.25. The aerodynamic resonance for separated flow has been noticed in NASA Ames data presented by Davis. Mabey has discussed flow instabilities over rigid, nonmoving, thick, biconvex airfoils at low angles.

Flutter model test results for a half-wing model show two transonic flutter speed dips. The lower speed dip occurs in attached flow with the flutter frequency close to the first (bending) mode as expected. The second dip, caused by the large changes in lift and moment, and the separated flow, occurs at a higher flutter frequency near the second (torsion) mode. The use of measured 2-D unsteady aerodynamic data, which include separation effects and information from 3-D steady tests in flutter analyses, predict the second torsional-buzz transonic dip.

Calculations were made using strong coupling between NLR's LTRAN 2 small perturbation method and Green's lag entrainment method for unsteady supercritical airfoil lift and moment data. These results agreed with test data much better than results from inviscid and weak coupling interaction methods as shown in Figure 4-4. Strong interaction viscous theory correctly produces a decrease in lift coefficient. Although viscous effects are too weak, the reversed sign of the lift phase angle is predicted as well as a point on the trend for the moment coefficient and its phase. Nonzero unsteady pressures at the trailing edge and the reversed shock motion shown in the tests were also predicted.

5. J. W. EDWARDS, S. R. BLAND, AND D. A. SEIDEL: "Experience with Transonic Unsteady Calculations"

The possibility of nonunique solutions for strong shock conditions was briefly discussed for several reduced frequencies.

The calculations presented are for inviscid flows although NLR viscous results were given for some comparisons. Methods used are the XTRAN2L 2-D and XTRAN3S 3-D small perturbation codes.

Steady and unsteady pressure distributions computed for the NACA 64A010 airfoil in pitch were in excellent agreement with experimental data for M = 0.50 and mean incidence of one degree. Agreement was also quite good for M = 0.796 where the computed steady flow shock was 2% too far aft and the unsteady peak was 10%-5% (as frequency increased) too far aft compared to measured values. Pressure differences are observable near shocks. Inviscid theory also predicted broader unsteady shock pulses with lower height due to shock movement as pitch amplitude increases in good agreement with experiment. Figure 5-1 shows the correct prediction of lift and moment coefficient trends with frequency. Viscous corrections improve agreements except for the imaginary part of lift due to pitch. Wall effects are expected at low frequencies.

Steady flow pressure calculations for the NACA 64A006 with oscillating flap show good agreement with experiment at lower Mach numbers. This is reflected in relatively good agreement with test data for predicted unsteady pressure distributions at M = 0.800 and 0.825. Separate unsteady shock pulse and hinge line singularity peaks are predicted. Both steady and unsteady calculated pressure distributions show differences compared to test data at M = 0.850 and 0.875. Trailing edge unsteady pressures agree with test data. Figure 5-2 shows the aerodynamic coefficients versus Mach number at a lower reduced frequency. Inclusion of viscous effects in theory generally improves agreement. Not shown in this summary is the much better agreement in unsteady coefficients and trends with Mach number at a higher reduced frequency of 0.24. This is due to the better agreement between calculated and experimental chordwise pressure distributions at the higher frequencies.

Inviscid unsteady calculations for the blunt leading edge, thick NLR-7301 airfoil oscillating in pitch at low Mach number (0.5) show reasonably good agreement with the experimental pressure distributions. Agreement was good for steady data although lower surface pressures were overpredicted. For the design point condition, the steady pressure distribution was not well predicted. The predicted chordwise unsteady pressure distribution shows features which are broadly similar to the experimental data so hope was expressed that viscous corrections in theory could show improvements. Both theory and experiment show the sensitivity of this supercritical airfoil to flow conditions.

The XTRAN2L inviscid small perturbation theory showed that reasonable and usable results could be provided below stall and separation (up to 8.5 degrees) for a NACA 0012 airfoil undergoing increasing angles from 0 to 15 degrees at constant rate. Instantaneous pressure distributions and lift agree reasonably well up to stall, which is delayed by a higher pitch rate. Figure 5-3 shows the good agreement between calculated and experimental lift coefficients at large angles. Moment coefficient data do not agree as well because of underprediction of loads near the leading edge and also separation for higher angles. Large second-harmonic components are present in moment coefficients and third harmonics are evident in Figure 5-3d.

Finally the results of comparisons between 3-D XTRAN3S (also a small perturbation method) data and test data were shown for a 12% supercritical, AR = 2, half-span model. Steady-state predictions were in reasonable agreement with test data at M = 0.70. Design Mach number is 0.8. The inviscid calculations showed poor agreement with test data for shock location at M = 0.825 so no unsteady data were shown. Figure 5-4 shows the unsteady results for M = 0.7. A viscous effect on the phase angle, due to lower surface pressures and geometry, is noticed at low frequency in test data. This effect disappears at higher frequency. The agreement between test and theory improves with increasing frequency and is better near midspan where shock effects are not overpredicted and tip effects are not pronounced. Agreement between calculated and experimental pressure distributions, both steady and unsteady, might be improved by the incorporation of better grids and viscous modeling.

Later calculations given in NASA TM 85817 show a broader 3-D shock pulse with increasing frequency in contrast to 2-D predictions.

6. D. J. SALMOND: "Calculation of Harmonic Aerodynamic Forces on Airfoils and Wings from the Euler Equations"

Since the Euler equations are the most accurate of inviscid methods and are likely to be more applicable for stronger shocks, lower aspect ratios, and higher sweep angles, the author extended these to subsonic-supersonic unsteady flows. The Pulliam and Steger steady flow method was used as a basis.

Applications of the fully conservative method were made to the NACA 64A010 airfoil in pitch. Steady calculations show very slightly different upper and lower pressure distributions due to slight asymmetry. For a lower reduced frequency, the agreement with test data for both real and imaginary parts of the first harmonic pressure distribution is good in front of and well behind the shock, but not as good at or near the shock. Results for a reduced frequency parameter of 0.404 are shown in Figure 6-1. Similar comments hold. The agreement for the real part is less good at an even higher frequency, but agreement between calculated and test data improves for the imaginary part.

Calculations are also made for the mid-semispan station of a very high aspect ratio wing and are compared with 2-D airfoil data. The 2-D and 3-D steady and unsteady results agree extremely well except for small differences near shock locations.

Subcritical flow calculations were made for the highly swept AGARD tailplane and are compared with experimental steady data in Figure 6-2 and unsteady data in Fig. 6-3. The full potential steady method (Arthur) and present Euler method data agree well with steady test data. The Euler method gives somewhat better agreement. Computed unsteady Euler results agree reasonably well with unsteady test data and are better than linear lifting surface results. (The frequency parameter is based on the root chord.)

Some new calculations for a free stream Mach number of M = 1.72 and frequency parameter of 0.543 were presented orally for pitch of the AGARD tailplane. Linear theory breaks down and results do not agree with test data especially near the leading edge region; the trend for the unsteady real part for the flat plate results is opposite to that of the Euler method and Mabey's test data near the airfoil nose. The real part from Euler results follows the experimental trend versus chord generally and agreement is better over the rear half of the airfoil. Flat plate unsteady imaginary components differ markedly in magnitude from test data, but Euler unsteady imaginary part results agree quite well with the experimental first harmonic chordwise pressure distribution. The leading edge is slightly supersonic at M = 1.72.

The unsteady calculations on the Cray 1S now take 2 minutes for 2-D calculations and 4 hours for 3-D calculations.

Future improvements will include implicit boundary conditions to permit larger time steps, will take advantage of characteristic directions, and will exploit improved grid locations and numbers. Flutter calculations will also be made for wings and conditions representative of industrial applications.

7. P. GIRODROUX-LaVIGNE AND J. C. LeBALLEUR: "Calcul D'Ecoulements Instationnaires Transsoniques Avec Decollements Par Interaction Visqueux-Non Visqueux"

A semiimplicit relaxation numerical technique having strong coupling for the interaction between inner viscous flow and outer small perturbation inviscid flow was described. It is consistent in space and time, and accounts for the downstream-upstream influence of viscous origins. Solutions of unsteady flows with shock-boundary layer interactions and with or without separation are possible. The (local) density of the mesh must be on a level or scale of the physical phenomena. Defect integral equations for the boundary layer and wake are closed by modeling the instantaneous velocity profiles and by a set of transport equations for the turbulence.

Applications of the 2-D method were made to airfoils. Very interesting figures were presented which portrayed instantaneous iso-Mach lines and boundary layer parameters.

Results are given for the thick NLR-7301 airfoil where the small perturbation assumption is stretched and where viscous interactions occur near the trailing edge. Predicted steady pressure distributions are in good agreement with the experiment except near the blunt nose. Shock location and intensity are reasonably well predicted. Upper surface instantaneous pressure distributions for airfoil pitch at M = 0.75 are also quite reasonably predicted throughout the cycle as are the compression and shock disappearance. Figure 7-1 shows the satisfactory agreement between predictions and test data for pressure derivative due to pitch and its phase.

Similar calculations were conducted for an oscillating flap. Steady lift and leading-edge moment coefficients were overpredicted compared to experimental data. Calculated unsteady first harmonic pressure distributions for flap oscillations are qualitatively similar to test data but the predicted peak is much higher near the shock. Predicted phase angles versus chord show a trend very similar to experiment except near the trailing edge.

Calculations were also made for the NACA 64A010 airfoil at 4 degrees incidence using two equations of transport. A finer mesh than previously employed was used in order to properly simulate flows with large viscous effects. Agreement between test and calculated steady pressures is improved for the plateau in front of the shock and also towards the trailing edge. Computed viscous parameters show extended separation from shock foot and reattachment in the wake. Test and calculated instantaneous pressure distributions correlate better. Figure 7-2 shows the rather good qualitative agreements during a pitch cycle.

The first harmonic pressure derivative for pitch versus chord is shown in Figure 7-3. The authors report that differences for separated regions aft of the shock have been reduced. The predicted shock is a little too far aft. The correct prediction of the phase changes near the shock is noticeable. The steady lift coefficient was well predicted while the leading edge moment coefficient was 16% overpredicted. The unsteady first harmonic lift modulus was 85% of the test value while the leading edge moment coefficient was 73% of the test value. Calculated phase angles differed from the test data by 5 degrees.

Thick, circular arc, symmetric, rigid, nonmoving airfoils have shown flow oscillations at intermediate transonic Mach numbers. Periodic shock movements, oppositely phased on upper and lower surfaces, occur. The reduced frequency based on chord is near 1.0. The authors qualitatively predict the oscillating character of the flow. Flow dissymmetry amplifies near separation and ends with moving shocks near 60% - 85% chord. The present calculations predicted a decaying oscillation with a noticeably different reduced frequency of 0.27. However, the most critical Mach number might be higher. Other investigations

are required before firm quantitative conclusions can be drawn. The method does seem to predict a complex unsteady flow phenomenon, the same as Navier-Stokes approaches do. The authors hope that contributions might be made to buffeting phenomena.

The method presented has also been applied in an approximate fashion to predict pressure distributions for a 15% split flap spoiler near mid-chord and displaced into the subsonic (M = 0.6) stream by 10 degrees.

The predicted steady pressure distribution across the chord is in surprisingly reasonable agreement with measured data in shape and magnitude. The results for spoiler oscillations are shown in Figure 7-4. For upstream locations, the unsteady pressure data are in good agreement. Large differences are noticed over the spoiler and downstream. The spoiler had only a few measurement stations. The second large predicted peak is not evident in the test data. The calculated phase angle is in good qualitative agreement with the test data.

Mr. LeBalleur later stated that extensions to 3-D would require modifications to the coupling technique, closure condition, and inverse method.

8. M. J. GREEN AND D. LAMBERT: "A Semiempirical Unsteady Transonic Method with Supersonic Free Stream"

Garner developed an economic, temporary, semiempirical method for predicting transonic oscillatory loads for industrial use. The method was reasonably successful in predicting the transonic velocity dip of a flutter model. The authors extend the method to supersonic free streams. The Allen-Sadler linearized theory for low aspect ratio wings in a supersonic flow is employed to provide information on velocity potentials and their spacial derivatives at zero and nonzero frequencies. Pressure data and their variation with angle are obtained from steady theory or experiment. An important mode such as pitch is used as a reference mode and a basis.

The method, using steady measured pressure data, is applied to a low aspect ratio, highly swept AGARD taileron whose leading edge becomes sonic at 1.55. For M = 1.32, a frequency of 70 Hz, incidence of zero degrees, and 65% semispan station, the unsteady real-part pressure distribution versus chord from theory agrees very well with experiment. The imaginary part does not agree quite as well. Both parts are better than linear theory. Figure 8-1 shows results at incidence for the 65% semispan station. Again, the real test and calculated components tend to agree well. While the imaginary parts show disagreements, the Green-Lambert predicted trend is correct and is much better than linear theory. The cross flow is small at this station.

Figure 8-2 shows a section close to the outboard side edge. While the agreement between real parts from the Green-Lambert method and experiment is good, the imaginary parts differ from test data at the aft end. The one-dimensional Bernoulli approach was replaced by a new formulation taking cross flow into consideration. Since flow directional properties are not practically obtained from measured pressure data, information from steady Euler approaches was employed for cross flow and pressure data. The unsteady pressure distribution computed by the revised method shows close agreement with that computed without cross flow for the 65% span station. Real and imaginary components, with and without cross flow, agree reasonably well with experiment at this station.

The rate of change of steady pressure coefficient with incidence across the chord computed by the Euler method for the tip station differs noticeably from measured data. The experimental data have a large peak near 15% chord and are noticeably lower than predicted values from 30% - 90% chord. These differences are reflected into the computed oscillatory data presented in Figure 8-3. The real part is not affected by cross flow. The cross flow corrections have significantly improved agreement of calculated data with experimental data for the imaginary part.

The authors believe they have overcome the major difficulties. More work to test the reformulated method with cross flow needs to be done. This method will be used to calculate generalized forces used in flutter analyses.

The use of Euler methods limits the procedure to flows without strong viscous effects.

9. W. J. McCROSKEY, P. KUTLER, AND J. O. BRIDGEMAN: "Status and Prospects of Computational Fluid Dynamics for Unsteady Transonic Viscous Flows"

In the review of the past progress, the authors point out a 10-year lag for developing unsteady codes after basic steady aerodynamic contributions are made. These lags are due to difficulties and complexities of performing time-accurate calculations at low frequency and the fewer scientists working in the area.

The improved paneling possible for steady subsonic flows has now been extended to steady supersonic flow and aircraft. TSP methods have been replaced by full potential and Euler methods for more complex geometries. An algebraic mixing length viscous model has been extended by Mansour to compute streamlines on a highly swept, low aspect ratio wing at 5 degrees incidence. Shock waves, tip vortex, separation, and reattachment zones were shown for the wing thereby indicating the great progress in steady 3-D Navier-Stokes methods. MacCormack's prediction is quoted that a Reynolds-averaged Navier-Stokes solution for a complete airplane will be obtained in 1985. In the viscous unsteady area, the

last ten years produced few engineering results of direct interest to the practicing aeroelastician. However, application of the 2-D Euler method and of the 3-D inviscid TSP method had been made. Progress can be judged by present achievements in unsteady 3-D full potential methods and 2-D Reynolds-averaged Navier-Stokes methods. Recently (1984), Horiuti et al. presented results shown in Figure 9-1 for an oscillating flap using Reynolds-averaged Navier-Stokes methods with simple eddy-viscosity modeling. Tunnel walls significantly affect the phase angles on the rear of the airfoil. The present authors stress the marginal capability in predicting the effects from ventilated-wall wind tunnels.

The paper discusses in detail the projections of capabilities in grid generation (including component-adaptive and solution-adaptive grids for bluff parachutes), grid spacing versus accuracy and stability, computer memory and speed, and also algorithm and solution methodology. The latter are more important in time-dependent problems where numerical instabilities arise.

Figure 9-2 gives estimates of CPU time for a wing with flap, simple body or store. As method complexity increases, maturity and confidence would decrease. TSP and full potential unsteady methods may be the most popular for the next few years. With advanced algorithms and computers, time-linearized methods seem practical for wide industrial use while thin layer (streamwise diffusion neglected) and Reynolds-averaged Navier-Stokes methods would likely be used for research, physical insight, or very critical problems. Dr. McCroskey expressed hope for the full potential method with integral formulation and also the Euler method with differential formulation for boundary layer effects. Figure 9-3 gives their overview of turbulence modeling. The authors point out that only viscous wedge, velocity profile (integral boundary layer), and zero-equation eddy-viscosity models have been used for unsteady flows up to now. It was expected that the two-equation eddy-viscosity model would be applied to aeroelastic problems in the near future and to flows with separation. (In Figure 9-3, W sub GT is the operations per grid point per time step.) The authors state that turbulence modeling is the weakest link, greatest challenge, and primary pacing item for both steady and unsteady flows. "Flutter calculations will only be as good as the viscous model," said Dr. McCroskey!

Vortical flow modeling was discussed, including that of Caradonna et al. who used concentrated vorticies in potential flow methods. Srinivasan and McCroskey prescribed a vortex but allowed it to develop its path in space. It has been used successfully for potential, Euler, and thin-layer Navier-Stokes analyses of unsteady airfoil-vortex interactions. [It will be recalled that V. J. E. Stark showed a 17% drop in flutter speed when leading edge vorticies were taken into consideration in a crude way (AGARD CP-226)].

Pre-, intermediate-, and post-processing of data will require improved graphic display technology and increased access time.

The last item touched upon research for, and use of, artificial intelligence or heuristic, knowledge-based, expert systems to proceed through a maze of possible paths and to interpret a large amount of data.

Final conclusions and recommendations made in the paper and presentation included exploitations of codes including user training and management indoctrination, code validation through selected experiments and calculation-test combinations, vortical flow modeling, nonlinear aerodynamic-structural coupling methods wherein finite difference methods are used for the flow and finite element methods are used for the structure, and turbulence modeling. Research on wind tunnel wall effects could be added to this list.

10. P. MULAK AND J. J. ANGELINI: "Amelioration et Extension d'une Methode de Calcul D'Ecoulements Transsoniques Tridimensionnels"

A variational principle of Bateman and the optimization of the pressure functional lead to the correct approximation for the small disturbance equation with consistent boundary conditions. The alternating direction implicit procedure is extended to wings of general planiform and provides jump conditions for swept shocks. Time linearization is used.

The method is applied to two 3-D wings. The first is a 30-degree swept, semispan wing with supercritical profiles and considerable twist. Calculations are made for the case of inboard oscillating (15%) flaperon. Calculated steady pressures for the wing with 1.44 degrees incidence and for the midflaperon station underpredict the height and width of the leading edge shock on the upper side. Near the mid semispan and outboard of the flaperon, the steady pressure peak height is correctly predicted, but the experimental peak is wider and the shock strength is higher. The nose peak pressure predicted for the 72% semispan station is higher than the experimental peak which is also wider. The predicted shock locations are slightly forward of the experimental ones. The predicted lower surface pressure distributions are consistently higher than the experimental ones across the span. The authors discuss boundary layer, turbulent vortex sheet, and shock-circulation effects as possible explanations for deviations. Figure 10-1 and Figure 10-2 show experimental and calculated unsteady pressure distributions at spanwise stations. Test data show the leading edge shock effects due to flap oscillations. Disturbances are amplified outboard. The calculated unsteady peaks are less pronounced and reflect the statements made for the steady case.

The second application was made to a highly swept, low aspect ratio F-1 model which was oscillated in pitch about a swept axis. Steady chordwise pressure distributions for various spanwise stations show reasonable agreement with test data. The latter indicate

separation near the trailing edge by the lower levels of pressure. Measured and calculated unsteady pressures for pitch oscillations are shown in Figures 10-3 and 10-4. The test data show fluctuations and several peaks. Theses are thought to be caused by effects from the rough wood leading edge and a tip restraint cable.

The authors conclude that the results are satisfactory for the extreme wing designs. They are investigating ways to improve predictions of shock location, strength and movement, and to include $\partial \phi/\partial y$ into the functional expression and the equation of continuity. In addition, the method will be extended to flexible modes and will be applied to a supercritical wing.

A CPU time of 7 minutes was mentioned for each steady or unsteady case for the calculations reported without program restructuring. Vectorial programming could reduce CPU time to 2.5 minutes.

11. M. H. L. HOUNJET AND J. J. MEIJER: "Application of Time-Linearized Methods to Oscillating Wings in Transonic Flow and Flutter"

Results from a hybrid, imbedded panel, time-linearized, modest cost methods are presented. FTRAN2 is a 2-D code using small perturbation theory and small disturbance boundary conditions. FTRANF solves the time-linearized full potential equation with complete boundary conditions and is applicable to thicker airfoils. FTRAN3 solves the time-linearized full potential equation with small disturbance boundary conditions. To relieve the small shock displacement restriction, for some calculations, the authors average steady flow fields for several angles to approximate shock trajectories with amplitude. Furthermore, a warning is given against direct comparison of measured shock peak shapes with calculated values since calculated characteristics are artificially related to shock trajectories by mesh width, etc. Peaks based on mean (averaged) steady flow field are thought "to be related to physical shock displacements plus additional artificial mesh related shock displacements." While further results might be needed for final judgements, this use of averaged steady flow fields gave more favorable results.

Application of FTRANF to a pitching airfoil (NACA 64A010) showed very good agreement with experiment for the chordwise pressure distribution at a subsonic Mach number (0.5). Mean (steady) flow averaging for M = 0.796 moves loading a little aft just downstream of the shock. Unsteady pressure distributions calculated by TSP FTRAN2, full potential FTRANF, and averaged-flow-field FTRANF, showed reasonable agreement with NASA Ames test data except near shocks. Figure 11-1 shows analytical and experimental trends of unsteady pressure distributions with frequency. Best agreement occurs at intermediate frequencies. Lift coefficient variation with frequency was reasonably well predicted. Quarter chord moment coefficients showed differences due to variations in measured and calculated unsteady pressure near the shock.

Applications of FTRAN3 to the LANN wing are shown in Figure 11-2 for various frequencies. Agreement with experiment is stated as acceptable. Difficulties were encountered with pressure pickups so caution was advised in interpreting integrated and some local loads. Calculated imaginary parts tend to agree with experiment. The subsonic lower surface should show better agreement. A model resonance is evident at a reduced frequency of 0.2. Frequency trends are predicted correctly. Spanwise distributions of the real oscillatory lift were overpredicted more on the lower side but seemed acceptable. Deficiencies decreased with increasing frequency. Computed spanwise distributions of unsteady moments showed poor agreement with experimental data throughout the frequency range.

Quasisteady calculations were made by FTRAN3 and steady-state XFL022 for the LANN wing. Calculated quasisteady chordwise pressures at three spanwise stations show reasonable agreement between the two prediction methods and with measured data at M = 0.82. Amplitude (incidence) effects are noticed in the data from tests from leading edge to the shock. Two shock peaks occur at the inboard station with a single bigger peak at the middle station. XFL022 predicts the two peaks at the inboard station better. These effects are seen in the low frequency unsteady pressure distributions shown in Figure 11-3 which also gives FTRAN3 results. Experimental and calculated results show some agreements. Peaks are underpredicted on the upper side but the initial warning about peaks should be remembered. The lower surface is subcritical.

To demonstrate industrial capability, flutter analyses are made for a fighter with tip missiles or inboard stores. FTRAN3 is used for unsteady transonic airloads on the wing only. The doublet lattice method provides unsteady airloads for other aircraft parts. With transonic effects on the wing, the predicted instability is less severe than that predicted by linear doublet lattice methods. Experimental data show a lightly damped mode. Calculations for other store cases also showed a more stabilized flutter boundary using transonic unsteady airloads on the wing.

12. J. B. MALONE, S. Y. RUO AND N. L. SANKAR: "Computation of Unsteady Transonic Flows About Two-Dimensional and Three-Dimensional AGARD Standard Configurations"

The XTRAN3, 3-D small perturbation code was applied to the LANN wing in pitch. The steady flow suction at the leading edge was underpredicted and caused differences between theory and experiment downstream to the shock. Calculated unsteady first harmonic pressures are shown in Figure 12-1. (k is based on mean aerodynamic chord.) Agreement with experiment is reasonable and better away from the shock.

The SUNTANS finite difference method for the 2-D full potential equation was used for airfoil applications. Boundary conditions were applied exactly on the instantaneous surface. The method is applicable to thick, blunt airfoils in inviscid flow from M = 0.1 to 1.2. Calculations were made for the NACA 64A010 airfoil at minus 0.10 degrees while the test angle was minus 0.21 degrees. Predicted steady pressures are in quite good agreement with experiment at M = 0.82, although the suction in front of the shock is overpredicted. Calculated lift coefficient magnitude and phase and moment coefficient magnitude variations with frequency are in excellent agreement with test data except at very low frequencies. Calculated moment coefficient phases versus frequency are about 10 degrees too high compared to test data. The 2-D SUNTANS was also applied to the oscillating flap on a NACA 64A006 airfoil. Steady pressure predictions at M = 0.875 are in reasonable agreement with test data. Suction levels forward of the shock are overpredicted while pressures are overpredicted aft of the shock. Theory predicted the irregular B-type shock behavior at k = 0.234, as shown in the tests. The shock disappears during part of the flap oscillation cycle. Unsteady chordwise pressure distributions at the same reduced frequency are quantitatively reproduced reasonably well, but the calculated unsteady shock pulses are 10% chord further upstream. Otherwise, agreement would be much better. The predicted steady shock was 2% - 5% chord more downstream than the experimental shock. Inclusion of viscous effects in theory could improve agreement with test data.

The SUNTANS 2-D code was also applied to the blunt, thick NLR-7301 airfoil. Steady inviscid theory provided a strong shock which was too far aft, thus viscous steady theory was used. Lower surface pressure predictions agree quite well with experiment, and upper surface predictions agree reasonably well with test data. The predicted shock position is reasonably close to the test location. Unsteady viscous approximations used the same transpiration velocities found in the steady viscous solutions and were held fixed during the unsteady calculations. Figure 12-2 shows the calculated, first harmonic unsteady pressure distribution which noticeably underpredicts the measured shock pulses. Predicted shock pulse locations and phase angles seem satisfactory.

The 3-D full potential code UPSIPWING was applied to the low aspect ratio, clean F-5 wing which has high leading edge sweep. For unsteady calculations, the flow tangency is "calculated at the instantaneous wing surface position, but applied along the original, or mean wing surface shape." The predicted steady pressure distribution for M = 0.8 (subcritical flow) agrees very well with test data. Agreement was also good for steady data at M = 0.90 except near the tip. For M = 0.95, theory predicted the shocks shown by the experiment on both upper and lower surfaces as well as the slightly more aft upper surface shock. For M = 0.8, the unsteady pressure distributions for sections along the span are quite well predicted. The real components of the first harmonic unsteady pressure show the drooped nose effects. Calculated data also correlate with test data reasonably well for M = 0.90 where linear theory would not apply. First harmonic unsteady pressure components for M = 0.95 are shown in Figure 12-3. The authors stated that the phase angles between real and imaginary parts are also predicted qualitatively for both upper and lower surfaces at M = 0.8 and M = 0.9. Inclusion of viscous effects into theory could decrease discrepancies with test data.

While F-5 steady and unsteady test data for the clean wing and wing-with-stores are not included in the SMP test selection cases, they present a valuable standard for evaluating and improving theories.

Recommendations were made for additional correlations to provide proven codes for the flutter engineer and for development of methods and grids to model complex surface-body combinations.

13. A. LAURENT: "Calcul D'Ecoulement Transsonique Instationnaire Autour D'Aile a Forte Fleche"

Variational principles are employed to define the transonic small perturbation equation and compatible limits. The local direction of flow and its sonic type are determined so calculations may be made in the physical plane without space transformations. The method* is an extension of 2-D Murman-Cole ideas to 3-D and is fully conservative. It uses an alternate direction implicit approach. It applies to highly swept, low aspect ratio wings with lateral flows. Calculations are reported for wings in pitch.

Mesh size investigations were applied to the F-1 tail. Differences are noticed near the shock and the leading edge, and they increase towards the tip.

Calculated steady chordwise pressures for several spanwise stations for an extremely low aspect ratio rectangular wing at M = 0.85 show good agreement with those from the Jameson, nonconservative, full potential method for regions forward of the shock. The nonconservative method gives shocks and compressions which are upstream of those from the conservative small perturbation method.

Steady pressure distributions computed for a rectangular wing with 30 degrees sweepback and NACA 0012 profiles show a sharp, thin, high supersonic zone near the wing tip. The shock is strong and located near the quarter chord point. For wing mid semispan, the supersonic zone is lower and broader. The shock is located at mid chord and is weaker. For the root, the supersonic zone is even lower and also more broad. The shock

* time linearized

is located near three-quarters chord and has a higher rate of compression than at mid semispan. The sonic line is near the leading edge. Instantaneous pressure distributions were calculated throughout a pitch cycle and show, most interestingly, the three kinds of shock motion found experimentally by Tijdeman. The stronger shock near the tip leads to a nondisappearing shock during pitch motion with smaller chordwise motion (Type A shock). The shock disappears during a large portion of the pitch cycle at the mid semispan station (Type C shock). At the root, the shock appears to move upstream during part of the cycle, disappears, and later reappears at the rear of the airfoil (Type B shock). The calculations show a 17% contribution from the second harmonics in the unsteady pitch moment coefficients.

Applications are made to the highly swept, low aspect ratio F-1 model. It had deficiencies such as leading edge roughness and a joint step, and sometimes a tip cable. Steady pressure distributions calculated for M = 0.9 (slightly transonic) show generally good agreement with test data for most spanwise stations except those near the tip. For strong transonic flow at M = 0.95, comparisons are debatable due to model deficiencies and trailing edge separation. However, calculated pressures agree reasonably well with test data in front of the shocks and for shocks near the leading edge. Unsteady pressures were calculated for M = 0.95, and results show more shock movement for 10 Hz than for 20 Hz. Unsteady first harmonic pressure coefficients for M = 0.95 are shown in Figures 13-1 and 13-2 for two spanwise stations (near 57% and 76% semispan). The general behavior of unsteady test and calculated results seemed more similar when test and calculated steady data agreed.

Calculated and test steady pressure distributions for several spanwise stations show very good agreement for a slightly supersonic Mach number of 1.02. The cable affects data at the tip. Agreement in calculated test data could be improved for the trailing edge regions by including viscous effects in calculations. Unsteady data were not shown. Flow field calculations were made for the NORA (F-1 tail) model at M = 0.95 and compared to test data having a slightly different tip. Figure 13-3 shows the local Mach number for the steady case. Calculations agree with test data rather well for shock locations and strength. Some of the differences between test and calculated values at the root of the wing may be due to wall effects. The undulating peaks in front of the shock seem to be predicted generally. The author states that the method is easily extensible to wings with stores. The examples demonstrated the strong non-linearities and 3-D nature of transonic flows.

14. P. M. GOORJIAN AND G. P. GURUSWAMY: "Unsteady Transonic Aerodynamic and Aeroelastic Calculations About Airfoils and Wings"

Development and applications of the NASA Ames 2-D ATRAN2 and 3-D ATRAN3S (XTRAN3S) are discussed. Both are for the small disturbance formulation. Many of the applications include viscous effects by the ramp and lag entrainment methods.

For the NACA 64A010 airfoil at M = 0.796, the viscous methods predict the steady shock location, the magnitude of the lift coefficient versus frequency, and the magnitude of the moment coefficient versus frequency better. Both inviscid and viscous methods overpredict lift and moment phase angles due to pitch at low reduced frequencies. The shock pulse peaks in the unsteady pressure loadings at various reduced frequencies are lowered, are moved upstream, and are in better agreement with measured data when viscous corrections are included.

Viscous corrections significantly improve agreements with measured upper surface steady pressures over an MBB-A3 airfoil. Calculations show very significant reductions in the heights and upstream displacements of real and imaginary unsteady shock pulses especially for the lag entrainment method at k = 0.1 and M = 0.756 for airfoil pitch.

Viscous wedge corrections were also applied to the NACA 64A006 airfoil with oscillating flap. The lag entrainment calculations required time steps that were too small. Correlations with measured unsteady pressure data were qualitatively improved at M = 0.853. Improvements were more noticeable at M = 0.877 and M = 0.879, and for higher reduced frequency. Calculations showed that the lift coefficient could be predicted using the first harmonic of unsteady pressures. Shock strength contained higher harmonics.

Applications to the NACA 0012 airfoil in pitch with large (2.5 degrees) amplitude were made using viscous corrections. The chordwise unsteady pressure loads which were predicted for eight time spots around the cycle showed rather good agreement with experimental data. Differences between inviscid and wedge calculations were small except near the shock. The formation of a strong shock and also the shock disappearance over part of the cycle were predicted.

No data for the blunt, thick NLR-7301 airfoil were presented since the calculations showed poor agreement with experiment. This airfoil was considered to have been outside the small disturbance limits.

A modified shear transformation for the grid was recently developed for application to highly swept wings of low aspect ratio. Applications were made to the F-5 wing in pitch. Calculated lower and upper surface pressures now showed major improvements in agreement with test data at M = 0.9, except near the nose, for four spanwise stations. Figure 14-1 shows the rather good agreement between calculated and measured unsteady pressures.

Unsteady aerodynamic loads were used in flutter analyses with various levels of success. Viscous ramp and lag entrainment methods were applied to a plunging-pitching NACA 64A010 airfoil. The lag entrainment correction produced the closest agreement with the trend of flutter speed versus mass ratio obtained using measured unsteady aerodynamic coefficients. However, the former gave flutter speeds which were 25% - 12% unconservative compared to the latter, which used measured coefficients, over the range of mass ratios from 50-250. Viscous corrections lowered the computed flutter speeds for high mass ratios.

LTRAN3 flutter calculations (inviscid) for a circular arc, AR = 5 wing at M = 0.715, show good agreement with experiment in both flutter speed and frequency for a mass ratio near 37. Linear methods show trends similar to LTRAN3 calculations as mass ratio is increased, but the linear methods show lower flutter speeds.

Flutter calculations were also conducted for a model of a Japanese transport with NACA 65A012 section. Results are shown in Figure 14-2. The lower Mach number side of and most of the transonic flutter speed dip are well predicted. No flutter was predicted for M = 0.85. Later verbal comments stated that linear theory and XTRAN3S flutter speeds agreed at lower Mach numbers and that viscous effects in calculations did not change the calculated boundary. Comparisons with flutter frequencies, amplitude ratios, and phases were not given.

Applications were made to a rectangular AR = 4 wing with NACA 64A010 section and for a high wing-air mass ratio. Flutter speed results are shown in Figure 14-3. Inclusion of viscous effects lowers lift coefficients and causes significant changes in the phase angle. A 10% increase in flutter speed results. The flutter frequency is near the first bending mode. Flutter characteristics could be predicted using first bending and first torsion modes.

Two bending modes and two torsion modes were used in the flutter analyses of a swept wing with MBB-A3 profiles. The incorporation of the second torsion mode caused a 5% drop in flutter speed.

The authors conclude that ATRAN2 and ATRAN3S are ready for practical applications where transonic small perturbation limits apply.

15. H. ZIMMERMAN: "The Application of Transonic Unsteady Methods for Calculations of Flutter Airloads"

Applications of the Angelini-Couston transonic small perturbation technique, the linear TSP method of Voss, Deslandes' Euler method, and the doublet lattice method, with and without corrections for aerodynamic center and lift curve slope, are made to an airfoil with pitch or plunge oscillations.

Steady pressure distributions for an MBB-A3 supercritical airfoil predicted by various methods show differences upstream of the shock, but the agreement between methods for M = 0.765 and M = 0.8 is generally satisfactory. Unsteady real and imaginary pressure distributions from TSP show higher peaks than linear TSP near the shocks for pitch. TSP shocks are more downstream at lower frequencies. The differences decrease with increasing frequency. The unsteady peaks for TSP methods and plunge motions are much higher than those from linear TSP and increase with frequency, perhaps unrealistically said the author, for M = 0.765.

Figure 15-1 shows pitch and plunge aerodynamic coefficients versus frequency. Results for the three methods converge at higher frequency except for moment due to plunge. Noticeable differences between TSP and linear TSP methods occur for the real part of moment due to pitch, real part of lift due to plunge, and especially for the imaginary part of lift due to pitch. Variations of numeric parameters can cause 10% changes in TSP results. Some unsteady Euler calculations were also made for M = 0.80 and an angle of minus 0.4 degrees, and show the same general trend for pitch and plunge coefficients with frequency as other methods do. TSP results agree better with Euler data.

Unsteady pressure distributions were calculated for linear TSP using steady velocity potentials from TSP or the full potential method. The differences between the two linear TSP unsteady pressure distributions were small.

Flutter calculations were conducted for a 2-D airfoil with two modes. The lower frequency mode was mostly plunge with a nodal point well in front of the leading edge. The second mode was essentially pitch. The modes were selected to grossly simulate wing bending and engine pitch modes of a transport wing. Two frequency combinations were used. One combination had lower frequencies for mode 1 (10 Hz) and mode 2 (30 Hz). The second combination had higher frequencies for mode 1 (40 Hz) and mode 2 (60 Hz), and a higher frequency ratio. Flutter calculations are shown in Figure 15-2 for M = 0.76 and an angle of 0.85 degrees and M = 0.80 for an angle of minus 0.4 degrees. Tunnel stagnation pressure at the flutter point is greater for TSP, corrected doublet lattice, linear TSP, and uncorrected doublet lattice methods respectively, for M = 0.76. The differences are noticeable. As tunnel stagnation pressure increases, the airfoil-air mass ratio decreases.

The more negative the imaginary part of lift due to pitch is, the more likely is the possibility of a "single degree of freedom flutter" with nearly the first bending mode and frequency. This occurs for the TSP results at the higher Mach number of 0.80. Euler-type calculations for this Mach number show flutter involving both mode 1 and mode 2. For both Mach numbers, the corrected doublet lattice method results give a neutral point stagnation pressure almost equal to that from linear TSP.

Flutter calculations for the higher combination of modal frequencies, 40 Hz and 60 Hz, show that the stagnation pressure for flutter is essentially equal for linear TSP and TSP results. The uncorrected doublet lattice method gives the same critical stagnation pressure, but the corrected doublet lattice method gives a much lower stagnation pressure. The author states that these behaviors could be due to variations of real part of lift due to pitch at low frequencies.

The effect of incidence was investigated for the flutter case with lower modal frequencies (10 Hz and 30 Hz). Critical flutter stagnation pressures versus incidence are shown in Figure 15-3. The TSP method shows the largest drop with incidence. Single degree of freedom flutter in the first bending mode occurs for the higher angles at both Mach numbers.

In the later discussion period, Mr. J. Edwards pointed out an unusual bending type instability that occurred during transonic wind tunnel testing of an aeroelastic model of the DAST-ARW-2 wing. Mr. Edwards also discussed possibilities of predicting this phenomenon.

Flutter analyses for other cases are obviously needed since this particular model may be oversensitive.

The author concludes by recommending that static aeroelastic deflections due to steady loadings be considered in predicting unsteady loadings. Also, the various angles possible in high speed flight should be investigated. He stated that time-linearized flow equations do offer advantages.

A comment was made to the author that viscous corrections could cause effects equal to the differences between the various inviscid methods presented. The author agreed and stated that investigations including viscous effects were planned.

16. K. ISOGAI: "The Development of Unsteady Transonic Three-Dimensional Full Potential Code and Its Aeroelastic Applications"

A two-step, semiimplicit, time-marching, finite difference method for solving the 3-D full potential equation in quasilinear form has been developed at the Japanese National Aerospace Laboratory. It employs the quasiconservative form of Jameson's rotated difference scheme to capture shock waves. Flow tangency conditions are satisfied on mean contours.

Applications to the highly swept, low AR NORA wing, with nose-up twist and NACA 63006 section, were made and are shown in Figure 16-1. The agreement between theory and experiment is reasonable.

Flutter calculations were made for a high aspect ratio, clean transport wing with nose-down tip twist using time integration of structural and flow equations. Six modes were used for structural responses which only consumed 1% of the total computing time. The flow equation computations required almost all of the time.

Computed steady-state pressures used a 2-D strip boundary layer correction which significantly improved the agreement with test steady pressure distributions for M = 0.8 as shown in Figure 16-2. The bottom of the transonic flutter dip occurs near this Mach number. The modified airfoil shapes and slopes found were then applied in unsteady calculations without inner-outer flow unsteady interactions.

The calculated and experimental flutter characteristics are shown in Figure 16-3. The stagnation pressure at flutter increases with angle of attack (possibly due to aeroelastic untwisting for swept wings as recently discussed by Gravelle, Honlinger, and Vogel at the September, 1984, ICAS meeting). *Flutter stagnation pressures and the dip are well predicted. Frequency is reasonably well predicted, but the large disagreement with experimental frequency at the lower Mach numbers could not be explained. Unsteady aerodynamic calculations were performed for a twisted wing simulating elastic and geometric twist angles at flutter statically. This modified rigid wing was oscillated in pitch at M = 0.8. Steady pressures show a shock on the lower surface at 15% chord and at 85% semispan. This is reflected in sharp peaks of real and imaginary unsteady pressures and is thought to be the cause of minimum dynamic pressure. A rapid rise in flutter dynamic pressure occurs with the expansion of the supersonic region with increasing Mach number.

(Japanese report NAL TR-726T mentioned success in predicting the flutter characteristics of the supercritical wing model tested by Farmer-Hanson of NASA.)

* flutter speeds can increase with incidence due to boundary layer effects.

The authors discussed a clever method for calculating static aeroelastic phenomena at a given Mach number and a given dynamic pressure using their time marching code. Velocity is decreased and air density is increased at constant dynamic pressure to produce low wing-air mass ratios. At high reduced frequencies, oscillatory wing responses damp rapidly with time to give converged static aeroelastic deformations. An example demonstrated the method.

Flutter calculations were also made for a transport wing with engines. The full potential code shows a large transonic flutter dip for Mach numbers just above 0.8 in the inboard wing torsion mode. Doublet lattice methods predict significantly higher speeds at the dip and are quite unconservative.

The author applies the full potential method to predict (a) steady-state pressures for the ONERA M-6 wing at M = 0.84, (b) unsteady lift and moments for a swept rectangular wing (flat plate) at M = 0.8, and (c) unsteady pressures for an inboard flap on an RAE swept tapered wing. The latter case is shown in Figure 16-4. The various data for the above cases are in reasonable to good agreement with other methods or test data.

The time domain calculations were also applied to simulate flutter suppression systems using active controls to eliminate the instability.

The author states that gust response, gust alleviation, and aileron reversal applications are straightforward.

Thus, the state of the art in Japan is quite high and appears ready for industrial flutter applications.

THE ROUND TABLE DISCUSSION

Five questions were proposed as listed next. A discussion of each question follows.

1. How is transonic flutter clearance done today in the aircraft industry?

The unsteady airloads used for safety-against-flutter evaluations are now computed from modified linear theories such as strip theory, kernel function, and doublet lattice methods for the subsonic region and supersonic kernel, harmonic gradient, supersonic parallelogram integration, and the conventional Mach box method for the supersonic regime. Transonic trends are estimated from correlations between flutter model test data and the linear theories. Final flutter calculations are made with quasisteady corrections for lift curve slope and aerodynamic center and other modifications to the theory.

In Europe, measured unsteady pressures are sometimes used to guide estimates of oscillatory airloads. Messieurs den Boer and Houwink of NLR used measured 2-D transonic unsteady airloads together with quasisteady 3-D corrections from steady tests (EQS method) to predict the two transonic flutter speed dips shown by experiments.

The Japanese National Aerospace Laboratory has had success in predicting the flutter speed of the Farmer-Hanson model and a model of a preliminary design of a Japanese transport. Their 3-D full potential code requires considerable computer times. Practical methods for clean surfaces now exist, even if long.

2. Will the emerging transonic CFD methods change the procedures?

The consensus was that these new methods will have a great impact on the flutter calculation process, but not in the near-term future.

Additional validations to establish the improved reliability by comparisons with test data are required for realistic industrial cases before the methods will be accepted by managers and, especially, by civilian and military approval agencies. Also, the total costs of increased computer times and engineering support must be minimized. Efficient engineering and preliminary design methods are required. Thus, the contribution of milestone developments and their acceptances are likely to be evolutionary.

The same general process consisting of flutter calculations at various design stages, ground vibration tests, stiffness tests, model tests, flight flutter tests, etc., will still be used. The flutter analyses will improve in accuracy and will increase with the intent of minimizing flutter model and flight tests.

A crisis could accelerate the acceptance and use of the new unsteady CFD methods.

3. How will transonic flutter clearance be done in five years?

Few significant changes are likely in the next five years. However, the new methods with quicker turnaround times are likely to be used for intermediate design particularly if margins of safety are small or inadequate. TSP and full potential methods may receive main attention.

4. How will transonic flutter clearance be done in ten years?

The consensus of both scientific and industrial representatives was that, beyond five years, the new unsteady CFD methods would be used extensively. The methods would have matured, been evaluated and validated, and gained acceptance.

No definite conclusions could be drawn about the impact of the new technology on flutter model tests. The selection of the number and kind of models will certainly be improved. Trade-off studies to evaluate free-flying versus cantilevered models could be conducted as well as studies to minimize wing-store cases in model and flight tests. However, development of new grids and methods to handle wing-stores, T-tails, etc., is required before a sharp reduction in model and flight tests is possible.

Theory shows marked effects on flutter characteristics due to surface angles, and these results are supported by some tests. However, other tests of wings up to 6 degrees show that the transonic flutter speed dip extends over a very narrow Mach number range and is not influenced strongly by the angle of attack.

Separation effects have strongly influenced the results of flutter model tests.

Flutter model construction (surface smoothness) and testing certainly has to be improved as emphasized by several papers.

No definitive and quantitative statements were made about reductions in flight flutter testing although hopes were expressed. Any reductions would be significant in view of the very high costs per hour of flight time. However, the added complications of the angle of attack effects for both attached and separated flow as well as the increase in potentially critical cases, due to improved accuracy of prediction methods, make estimates difficult.

5. What are the research needs for the next five years?

Several opinions were expressed about the adequate state of the art for airfoils and available unsteady test data. Suggestions were made to conduct future tests on small 3-D models to decrease wind tunnel interference and to investigate realistic configurations.

Some research needs in the model area are:

1. Two-dimensional plunge-pitch flutter tests at various angles or lift coefficients.
2. Unsteady airload measurements over flexible models.
3. Prediction of flutter characteristics corresponding to Reynolds numbers at flutter model conditions and also for full-scale flight Reynolds numbers.
4. Comparison of flutter model data obtained at low Reynolds numbers and those obtained in new high Reynolds number facilities. Perhaps this can be accomplished through a cooperative program.
5. Wall and tunnel resonance effects on unsteady aerodynamics and flutter measurements.
6. Improved flutter model construction techniques and more careful test conditions.
7. Unsteady pressure measurements at high Reynolds numbers.

Analytical research needs include:

1. Grids and methods for surface-bodies, T-tails, etc.
2. Viscosity.
   a. Improved turbulence modeling.
   b. Continued development of semiempirical viscous methods for 3-D wings and extension of separated flow methods to 3-D.
   c. Extension of Navier-Stokes methods to buffet phenomena.
   d. Investigation of problems of fighter aircraft during high angle, maneuvering, transonic combat.
   e. Further studies of self-induced flow instabilities over rigid, nonmoving airfoils.
   f. Methods to predict wing torsional buzz and swept-wing bending buzz at higher angles.
   g. Methods to predict vortical flow effects on flutter.

3. Nonlinearities.

Methods for the simultaneous time integration of strongly nonlinear structural, unsteady aerodynamic and electrohydraulic elements (stability analyzed in the time domain as compared to the frequency domain).

4. Application needs:
   a. Selection of standard AGARD SMP industrial-type flutter cases and model test results.
   b. Investigations of simplicity versus utility versus computer times in various transonic unsteady airload methods by application to realistic cases.
   c. Training of flutter engineers.
   d. Indoctrination of civilian and military approval agencies in the new techniques.

CONCLUSIONS AND RECOMMENDATIONS

1. The new unsteady transonic CFD methods with their more realistic simulation of transonic physical phenomena are vital for improving accuracy in flutter predictions.
2. The AGARD cooperative program on transonic unsteady aerodynamics and aeroelastic applications has certainly stimulated excellent contributions and advanced the state of the art.
3. General conclusions on the state of the art seem to be:

   a. The various methods predict subsonic unsteady pressure distributions equally well.
   b. Unsteady pressure distributions for conventional airfoils are quite well predicted by inviscid methods at lower transonic Mach numbers and for attached flow. The agreement with test data deteriorates with increased angle and shock strength. Viscous corrections improve agreements as do increased frequencies. Lifts are better predicted than moments.
   c. Agreement of predicted unsteady data with test data is better when steady pressure data agree.
   d. Supercritical airfoils are very sensitive to flow conditions and require viscous corrections to improve agreement with test data. Some of the simpler TSP methods fail to adequately predict unsteady loads for blunt, thick surfaces.
   e. Viscous corrections are essential to even qualitatively predict unsteady aerodynamic pressure trends due to oscillating trailing edge flaps. The state of the art is fair, at best, and further improvements are needed for active control applications.
   f. Separated flow drastically changes the variations of unsteady pressures and phases with frequency. Flutter characteristics are altered significantly. Applications of new strong coupling-viscous methods predict the correct trends for 2-D airfoils. No 3-D methods for separated unsteady flow are available.
   g. Research on unsteady turbulence modeling and on wall effects requires high priority attention.
   h. Three-dimensional methods for predicting unsteady airloads for transonic flutter analyses of clean wings are now available even if lengthy and tentative. Methods for interfering surfaces-bodies are needed.
   i. Economic methods for preliminary design are needed.

4. Liaison between unsteady CFD scientists and flutter engineers must increase as well as training for the latter.
5. The tremendously useful data produced by the SMP cooperative program certainly requires continuous collation.
6. Application of the new methods by industrial flutter engineers should be presented at AGARD meetings and also national group meetings to accelerate transition of this more accurate and vital technology.

ACKNOWLEDGMENTS

Special thanks are due to:

1. Messieurs H. C. Garner (U.K.) and N. C. Lambourne (U.K.) for their most helpful input to this summary report.
2. Messieurs H. C. Garner (U.K.), N. C. Lambourne (U.K.), J. J. Angelini (France), J. Becker (Germany), and R. F. O'Connell (U.S.A) for their stimulating comments and lively participation in the Round Table Discussion.
3. Messieurs R. J. Zwaan (Netherlands) and J. W. Edwards (U.S.A) for their additional presentations during the Round Table Discussion.
4. Dr. Edward S. Wright, Director, Army Materials and Mechanics Research Center, Watertown, Mass., U.S.A., for arranging for typing and artwork, and to Ione Haines, Diane Valeri, Nancy Fleming, Marion Gould, and Sharon Ross for expedient and skillful preparation of this report.

1. "Transonic Unsteady Aerodynamics and Its Aeroelastic Applications," AGARD SMP CP-374.

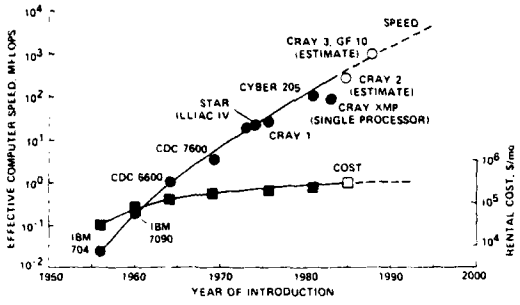

Figure 1-1. Growth with time of computer speed and cost.

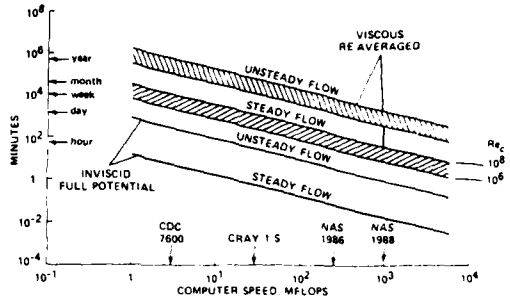

Figure 1-2. Times required to compute steady and unsteady flows about wings - 1984 algorithms.

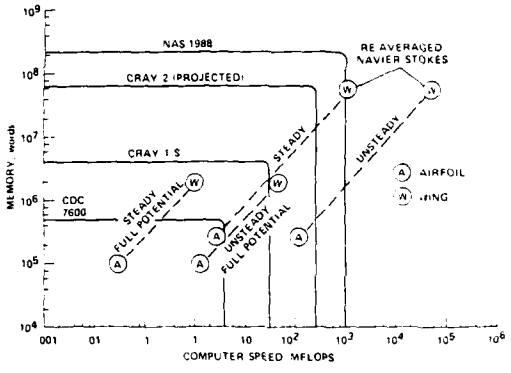

Figure 1-3. Computer speed and memory requirements for aerodynamic calculations - 15-minute runs using 1984 algorithms.

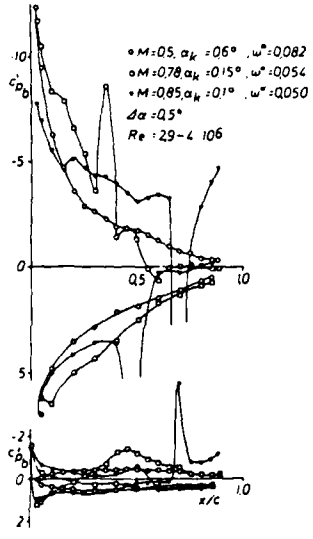

Figure 2-1. Effects of Mach number. Pitch oscillation about the c/4 axis.

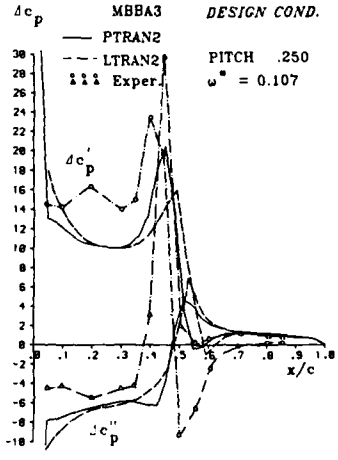

Figure 2-2. Two-dimensional unsteady load distributions - (CT3).

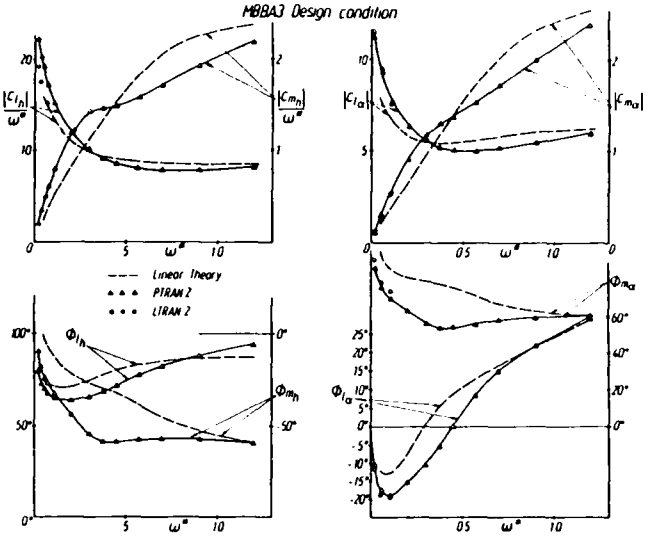

Figure 2-3. Frequency dependence of unsteady lift- and moment- (about c/4) coefficients due to pitching and heave motion.

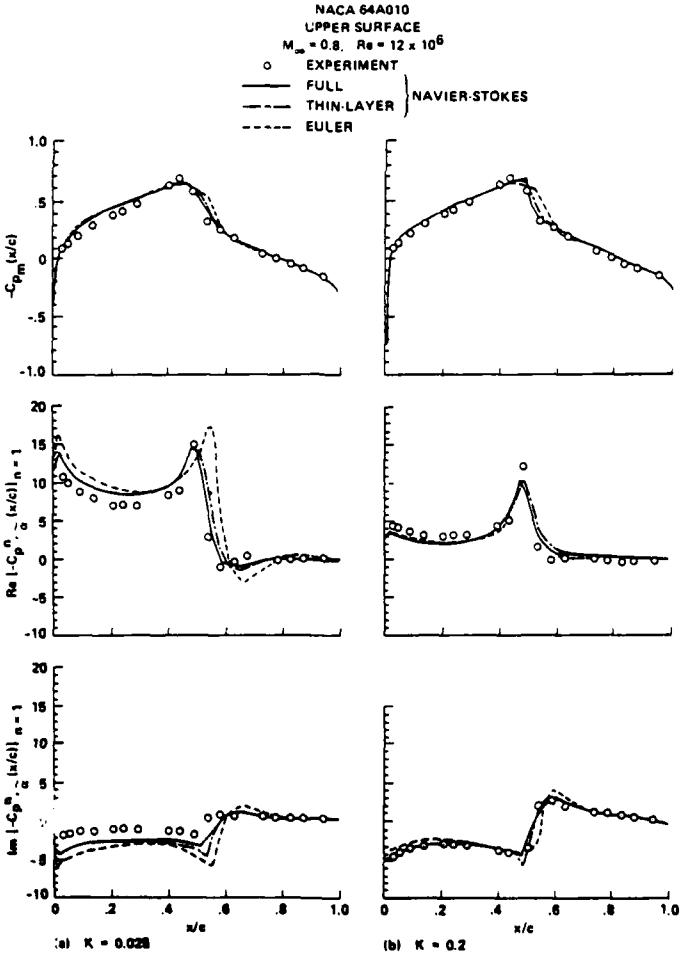

Figure 3-1. Mean and first harmonic complex components of pressure coefficients: $\alpha = 0^0 + 1^0 \cos \omega t$.

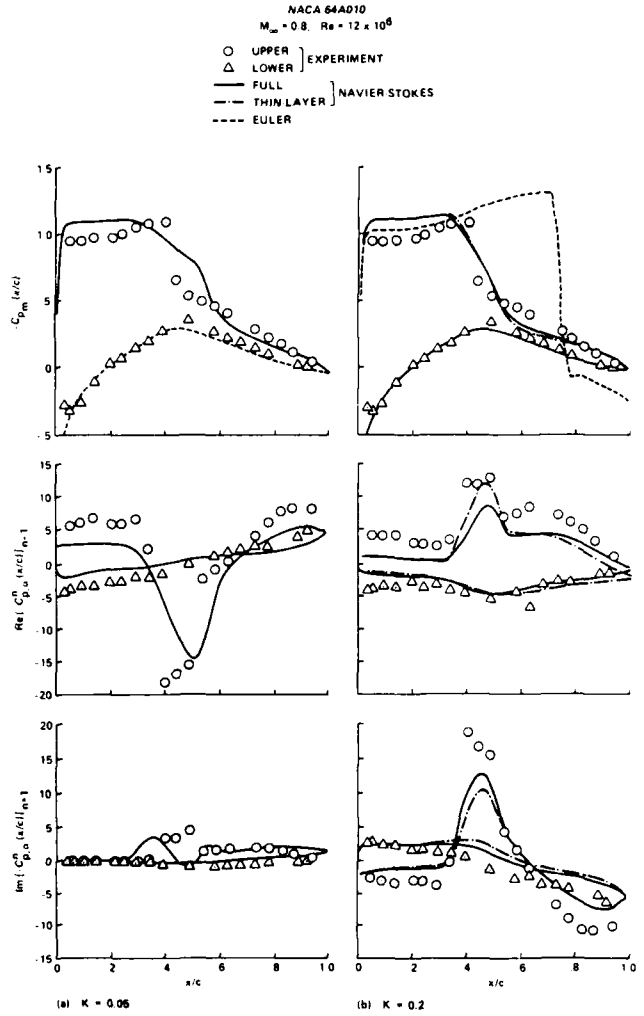

Figure 3-2. Mean and first harmonic complex components of pressure coefficients: $\alpha = 4^\circ + 1^\circ \cos \omega t$.

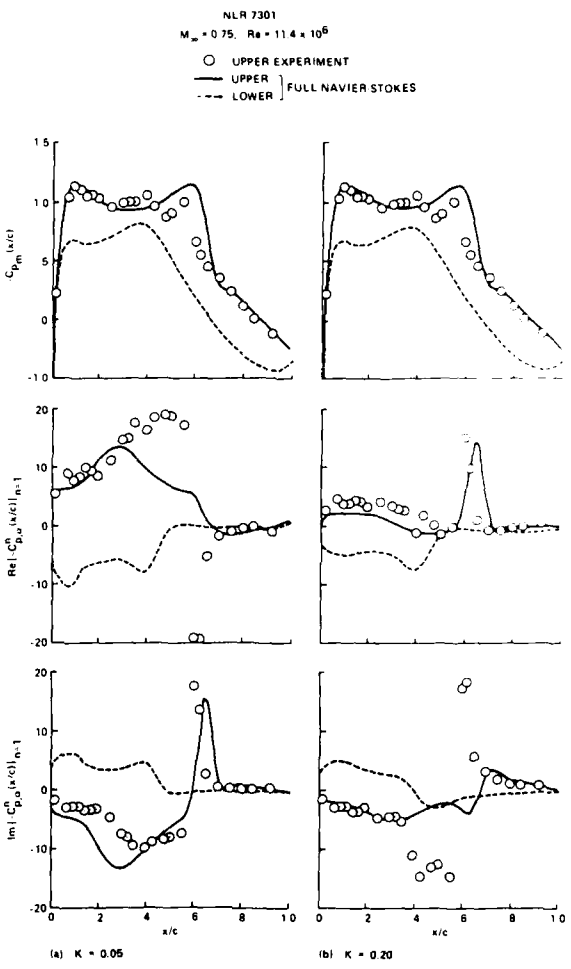

Figure 3-3. Mean and first harmonic complex components of pressure coefficients: $\alpha = 0.37^\circ + 0.5^\circ \cos \omega t$.

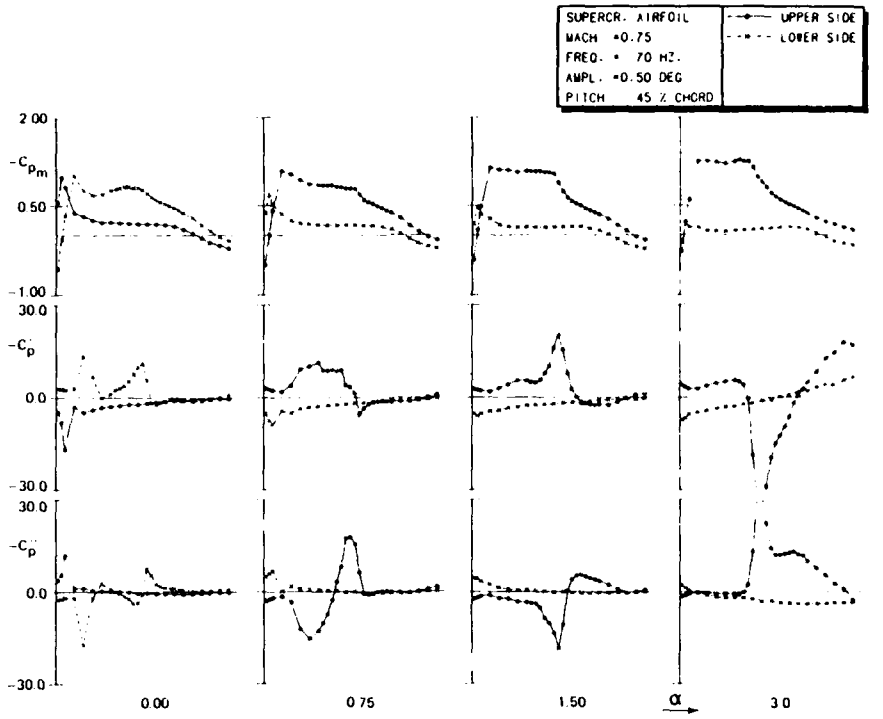

Figure 4-1. Mean and unsteady pressure distribution at four incidences.

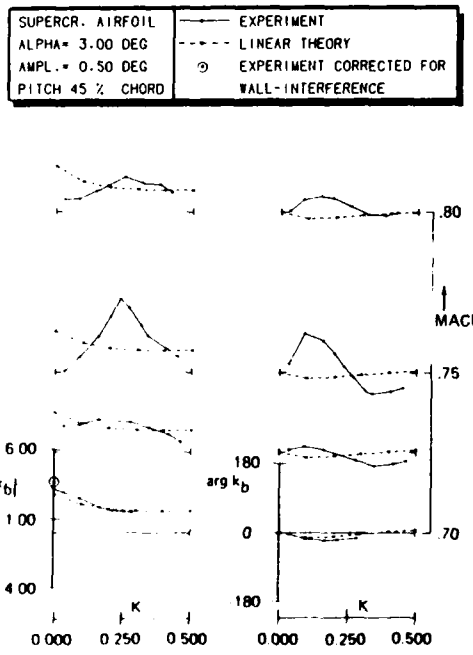

Figure 4.2 Influence of reduced frequency on unsteady lift coefficient, at various Mach numbers.

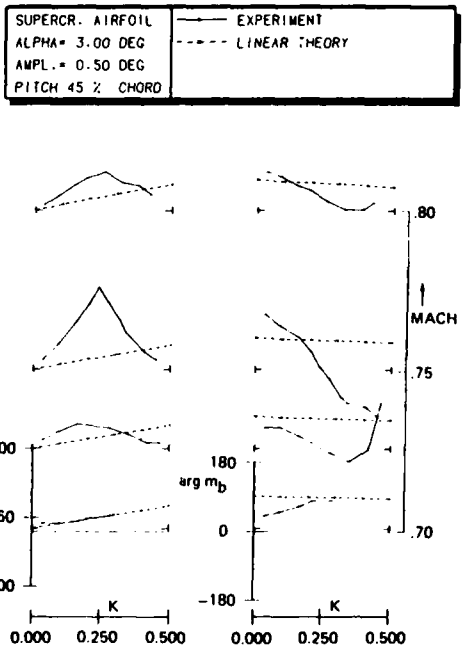

Figure 4-3. Influence of reduced frequency on unsteady moment coefficient, at various Mach numbers.

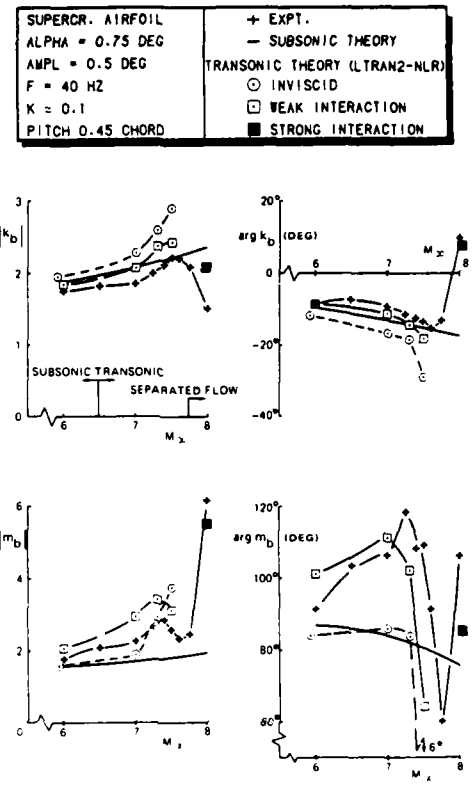

Figure 4-4. Unsteady lift and moment coefficients on an *oscillating supercritical airfoil.*

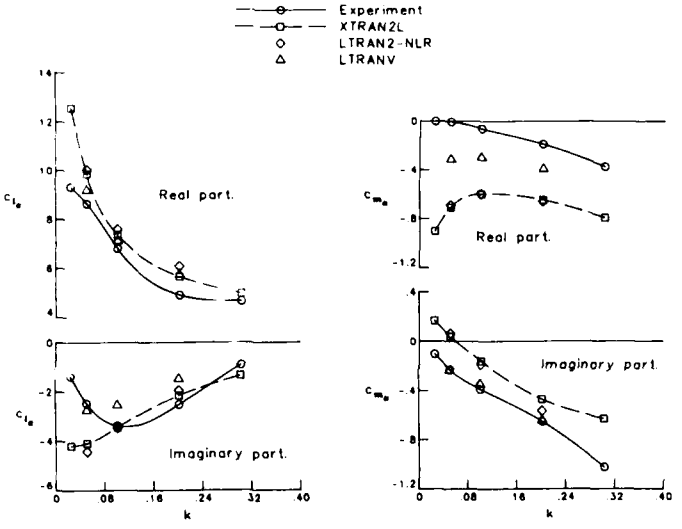

Figure 5-1. Comparison of unsteady forces for the NACA 64A010A airfoil at M = 0.796, $\alpha_0 = 1^0$ (CT 3-7).

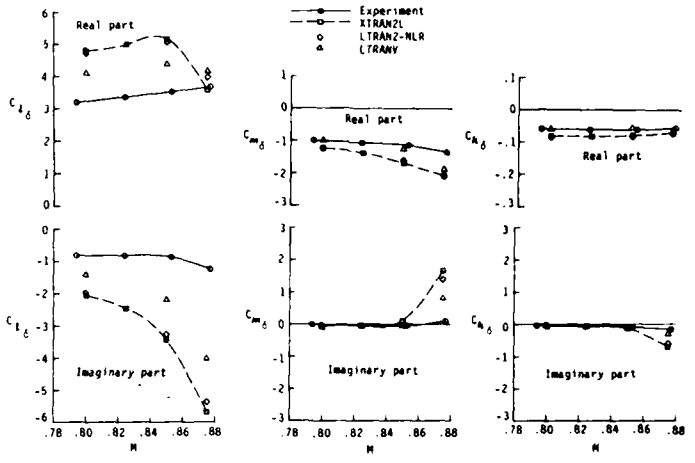

Figure 5-2. Comparison of unsteady forces for the NACA 64A006 airfoil at $\delta_0 = 1^o$, k = 0.06 (CT 1, 3, 6, 8).

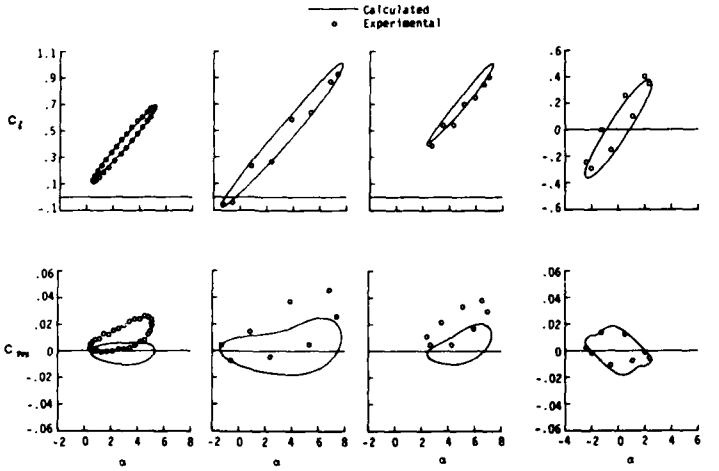

(a) $M = 0.6$, $\alpha_m = 2.89^o$ (CT 1) $\alpha_0 = 2.41^o$ (b) $M = 0.6$, $\alpha_m = 3.16^o$ (CT 2) $\alpha_0 = 4.59^o$ (c) $M = 0.6$, $\alpha_m = 4.86^o$ (CT 3) $\alpha_0 = 2.44^o$ (d) $M = 0.755$, $\alpha_m = 0^o$ (CT 5) $\alpha_0 = 2.51^o$

Figure 5-3. Comparison of unsteady forces for the NACA 0012 at k = 0.081 (CT 1-3, 5).

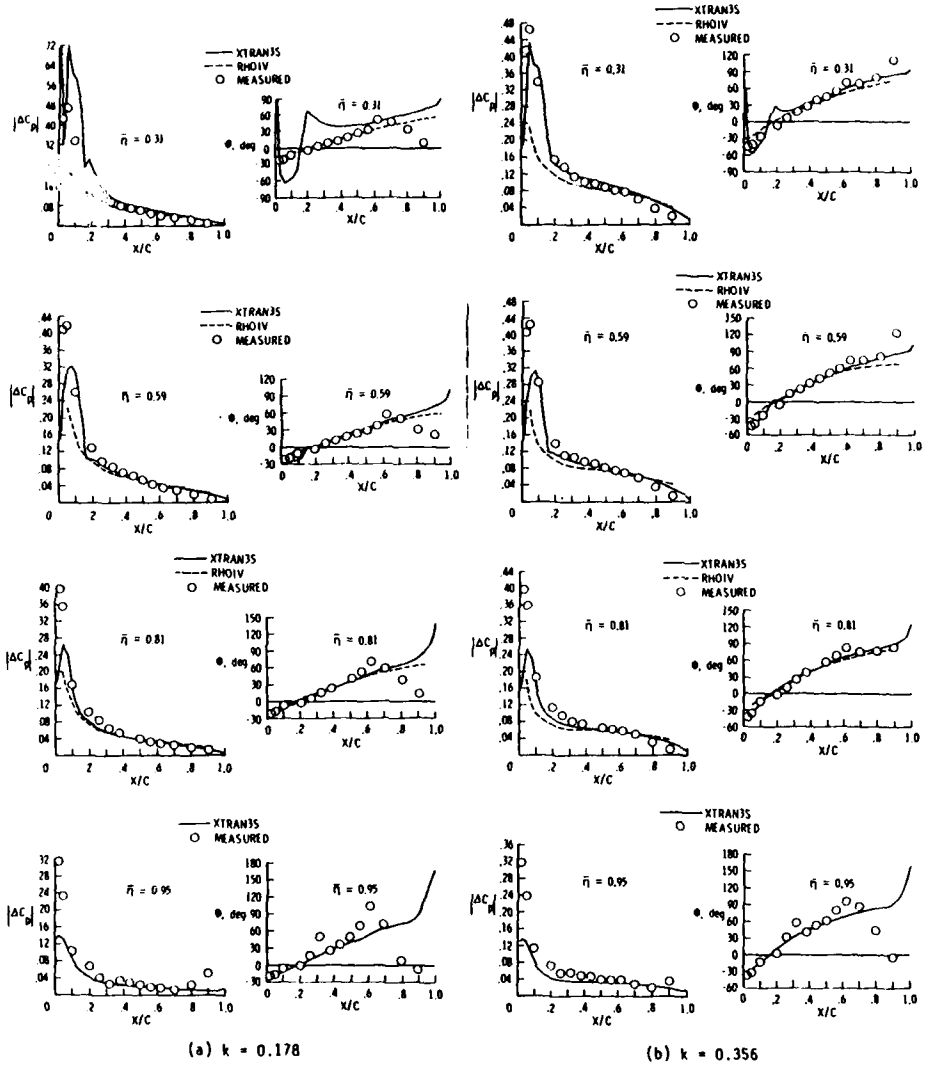

Figure 5-4. Comparison of measured and calculated unsteady pressure distributions for rectangular supercritical wing at M = 0.7, $\alpha_m = 2^o$, $\alpha_o = 1^o$.

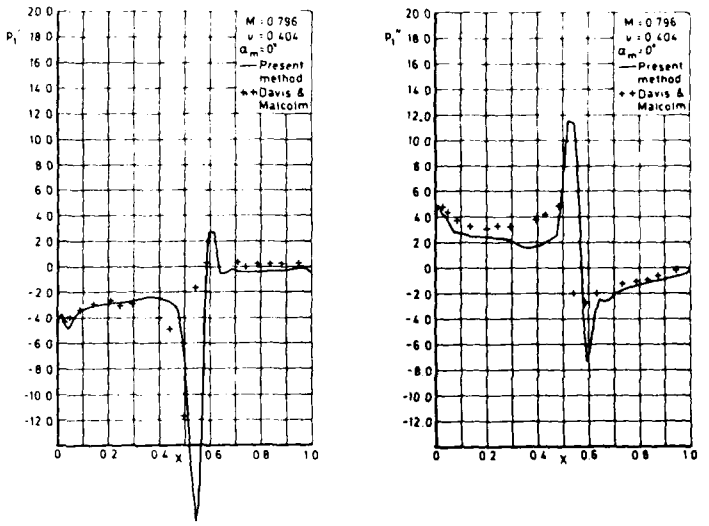

Figure 6-1. In-phase and in-quadrature parts of first harmonic pressure distribution for oscillation in pitch about the quarter chord of NACA 64A010 (Ames model).

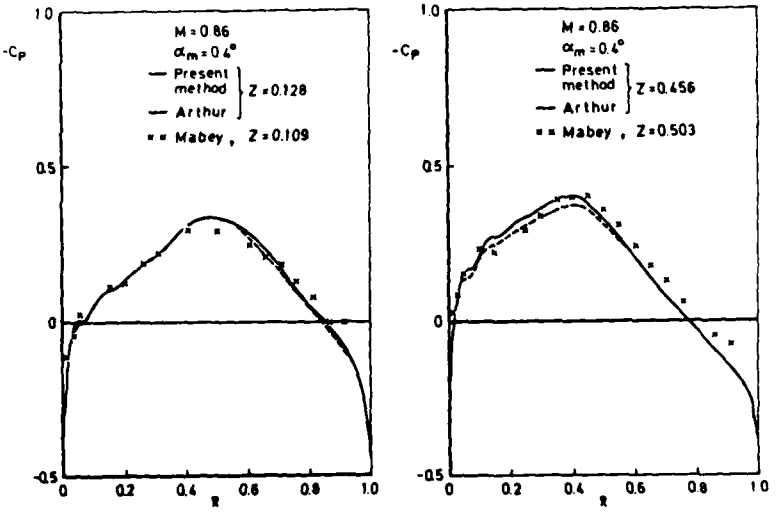

Figure 6-2. Steady pressure distribution for AGARD tailplane.

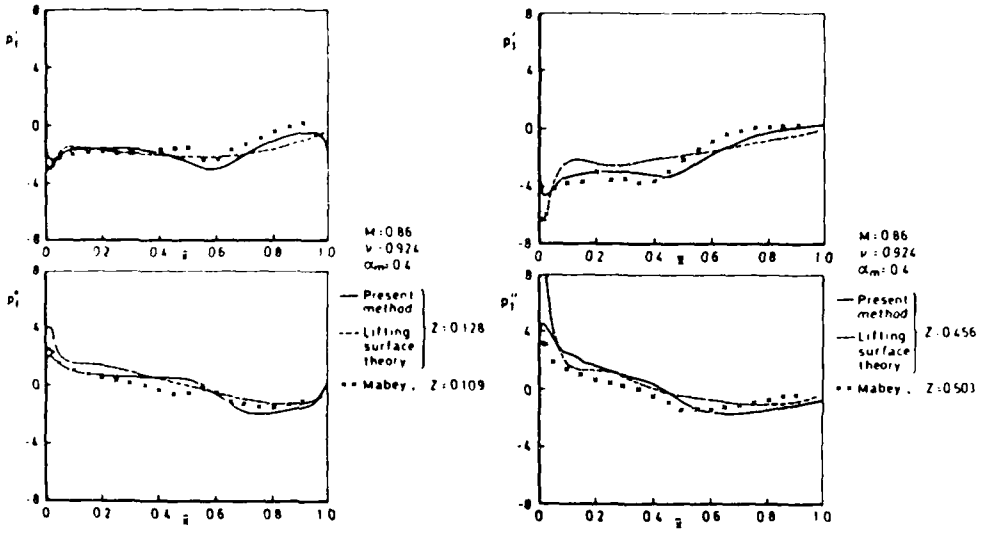

Figure 6-3. In-phase and in-quadrature parts of first harmonic pressure distribution for oscillation in pitch of AGARD tailplane.

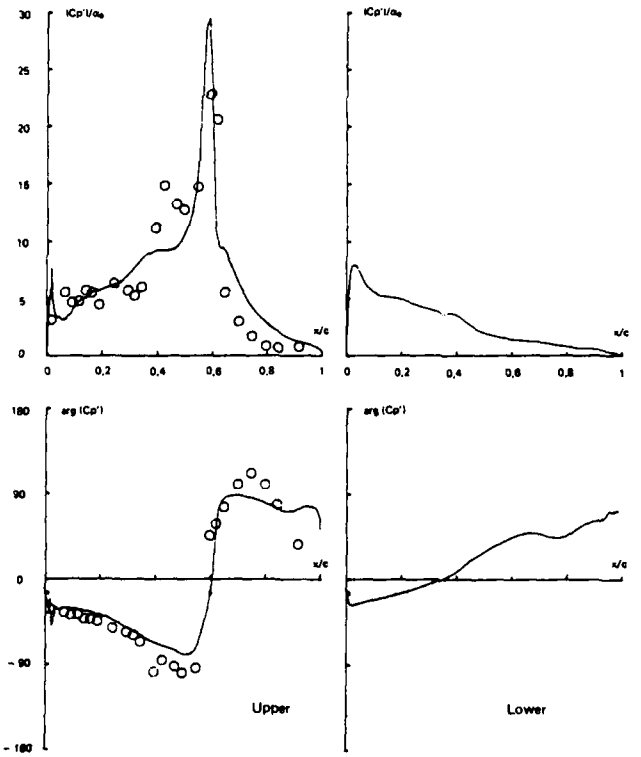

Figure 7-1. Profile NLR 7301. M = 0.75; $\alpha = 0.37^{o} - 0.5^{o} \sin \omega t$; Re = 11 x 10^{6}, k = 0.40. First harmonic of pressure coefficient. (Calculated---, test NASA Ames o o o o).

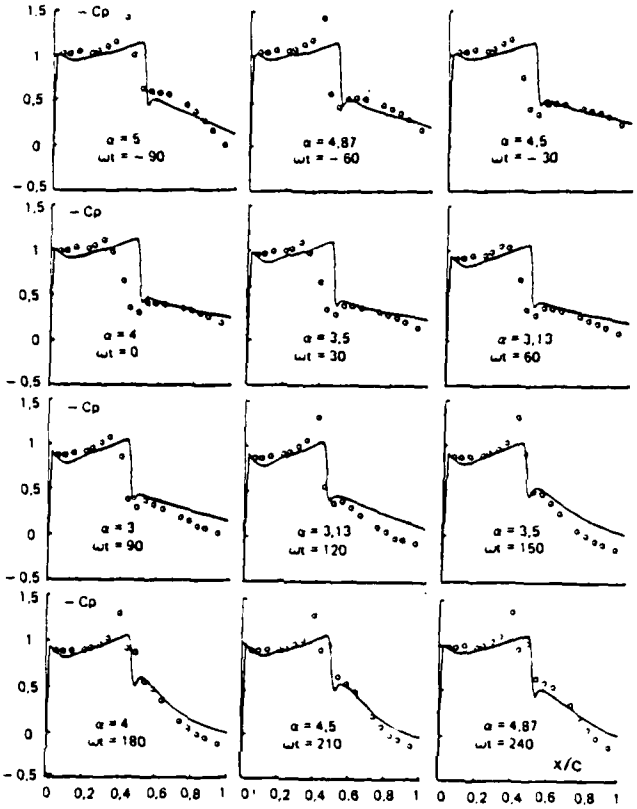

Figure 7-2. Profile NACA 64A010. M = 0.789; α = 4° · 1° sin ωt; Re = 12 x 10⁶; k = 0.40. Instantaneous pressure coefficient. Upper surface. (Calculated---, test NASA Ames o o o o).

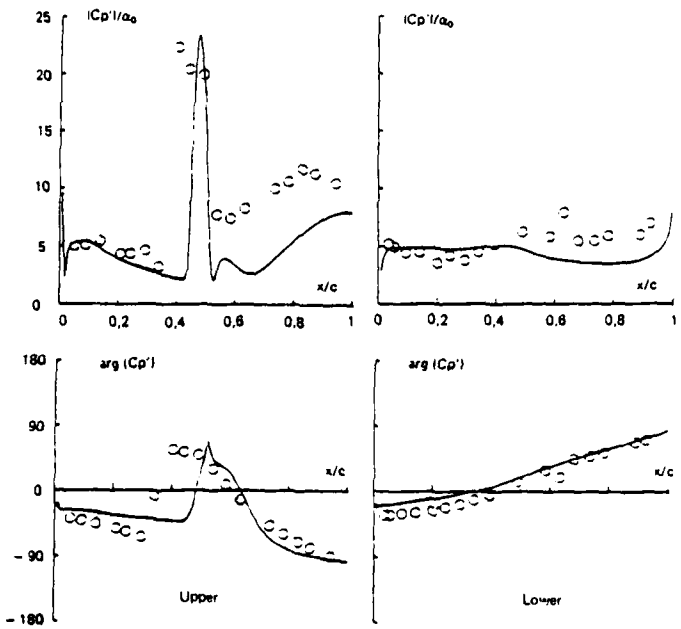

Figure 7-3. Profile NACA 64A010. M = 0.789; α = 4° · 1° sin ωt; Re = 12 x 10⁶; k = 0.40. First harmonic pressure coefficient. (Calculated---, test NASA Ames o o o o).

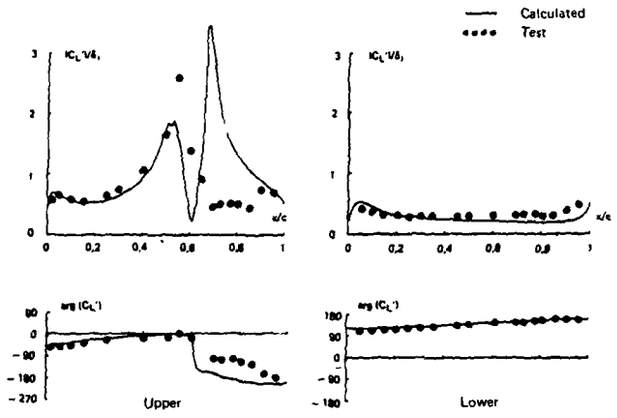

Figure 7-4. *Profile* RA 16SC1 with oscillating spoiler. First harmonic of pressure coefficient. ($M = 0.06$; $\alpha_m = 0^o$; $Re = 4 \times 10^6$; $\delta_{sp} = 10^o \cdot 1^o \sin \omega t$; $k = 0.30$).

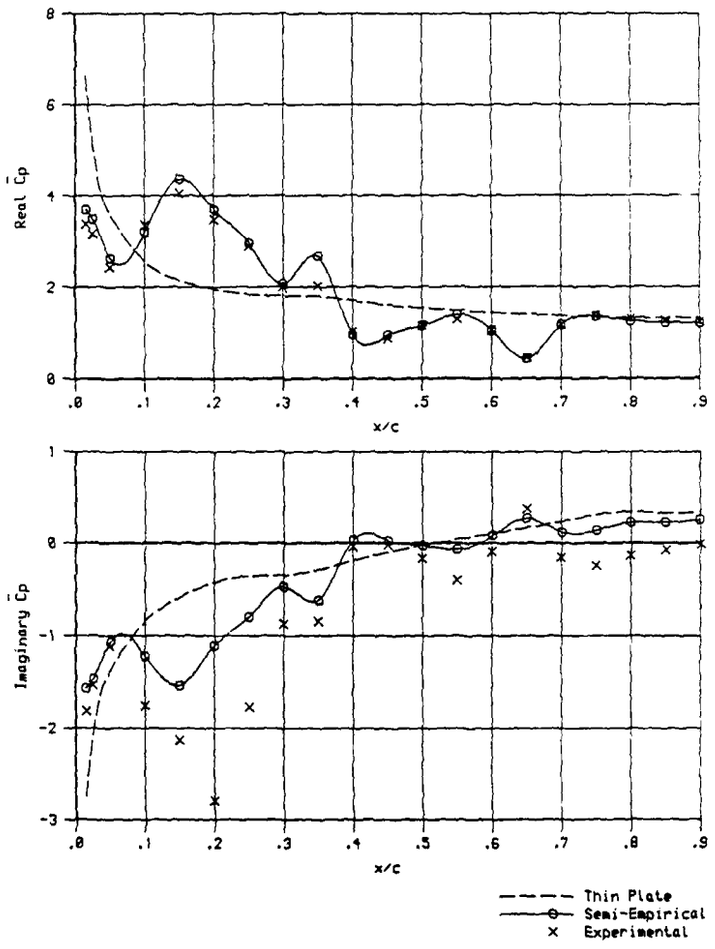

Figure 8-1. Oscillatory lower surface pressures, Section 3, M = 1.32, Frequency (Hz) = 70.0, Incidence = -5.0.

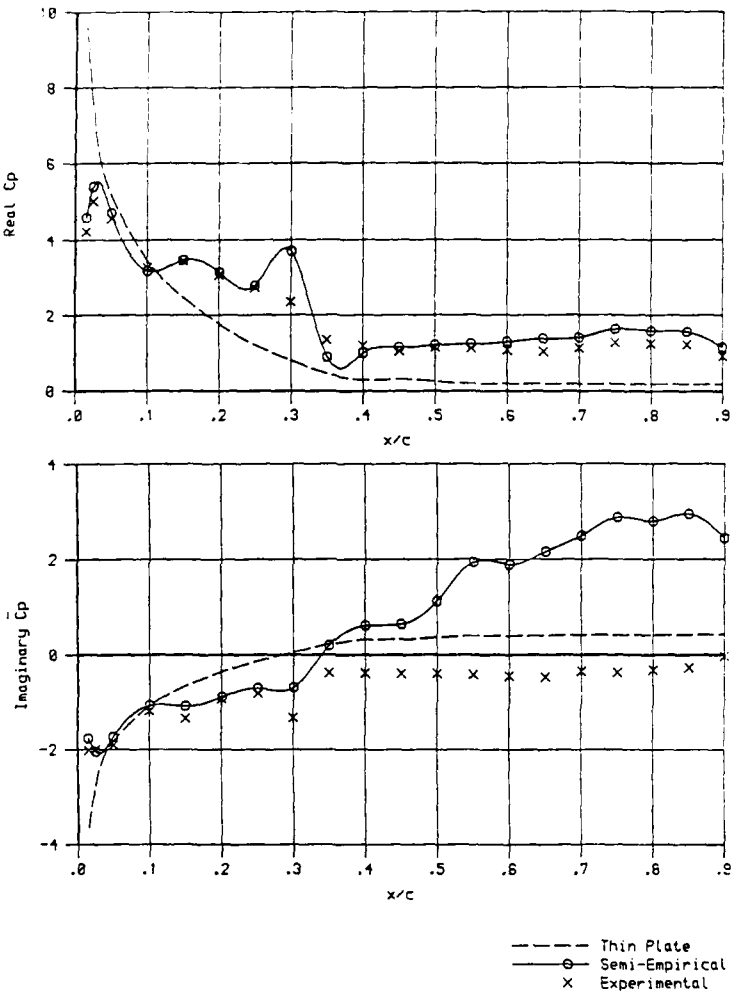

Figure 8-2. Oscillatory lower surface pressures, Section 5, M = 1.32, Frequency (Hz) = 70.0, Incidence = -2.0.

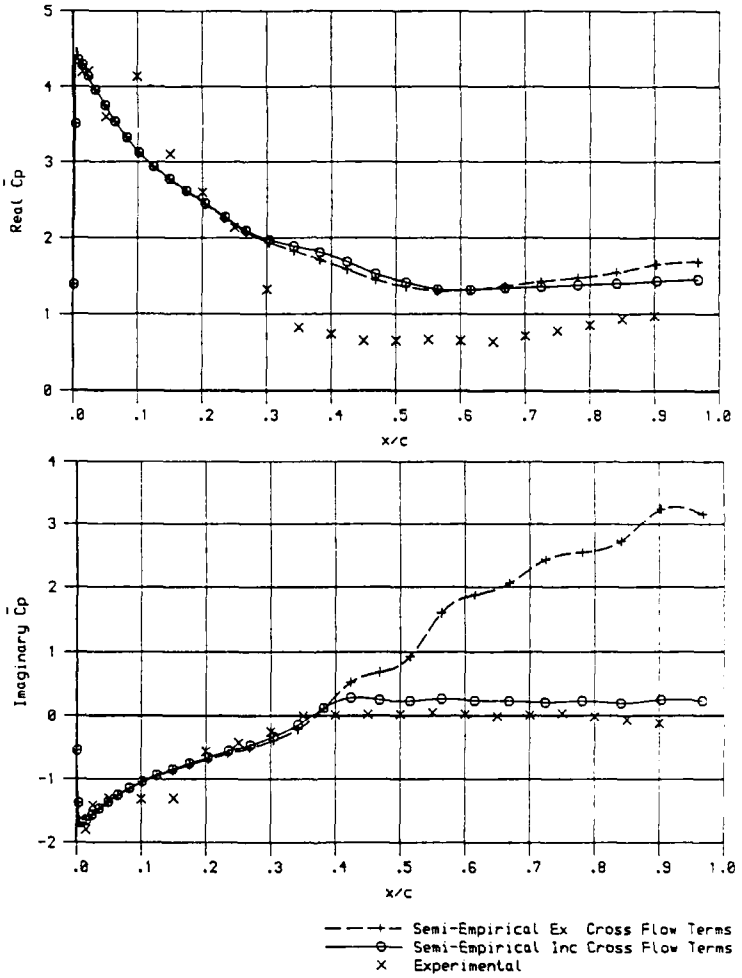

Figure 8-3. Oscillatory lower surface pressures, Section 5, M = 1.32, Frequency (Hz) = 70.0, Incidence = 0.0.

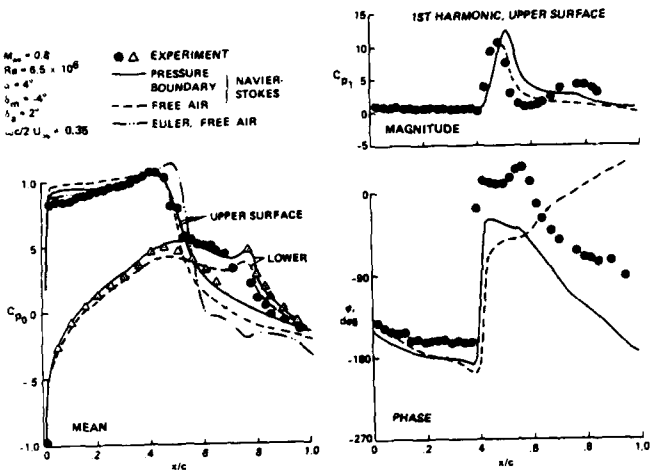

Figure 9-1. Transonic viscous flow over an airfoil with an oscillating flap.

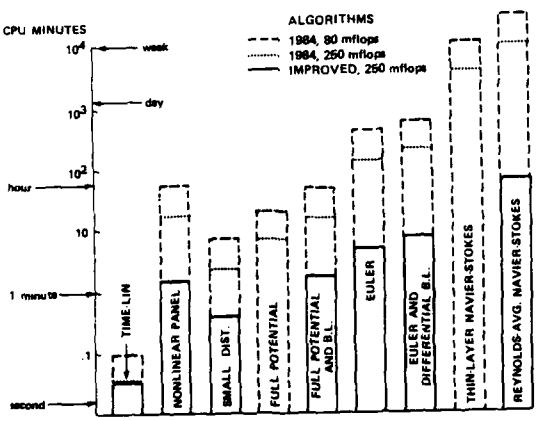

Figure 9-2. Solution times for a wing of moderate complexity; 75 chords travel/case, improved algorithms, 250 mflops.

Model	Physical Generality	Numerical Compatibility	Remarks
Viscous wedge	Very low	Very high	Shock-B.L. interaction
Integral B.L.	Low	High	Very good when highly tuned
Eddy viscosity			
Zero eqn	Low	High	Needs more tuning
.			
.			
2-eqn	Medium	Low to high	ΔW_{GT} = 20%, $\Delta\tau$ = ?
Reynolds stress equations	High	Low	3-D separation?
Large eddy	Very high	Low (?)	Guidelines for above
Complete simulation	Complete	nth generation supercomputers	

Figure 9-3. Turbulence models.

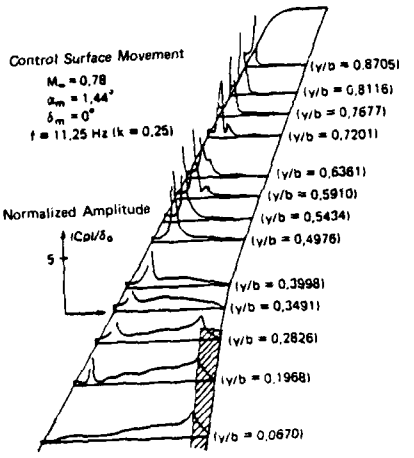

Figure 10-1. Distribution of unsteady experimental pressures (upper) at spanwise stations.

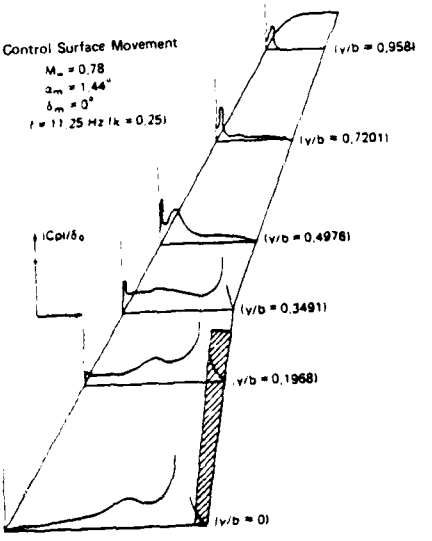

Figure 10-2. Distribution of calculated unsteady pressures (upper) at spanwise stations.

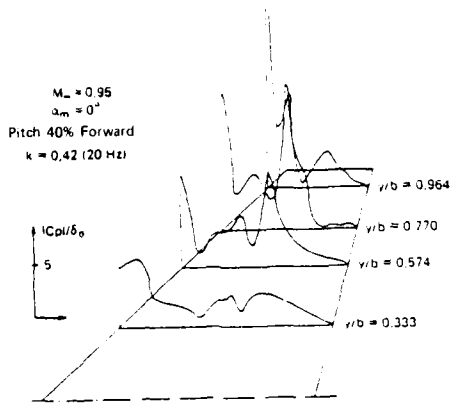

Figure 10-3. Distribution of experimental unsteady pressures at spanwise stations. Normalized amplitude/Cpl/α_0.

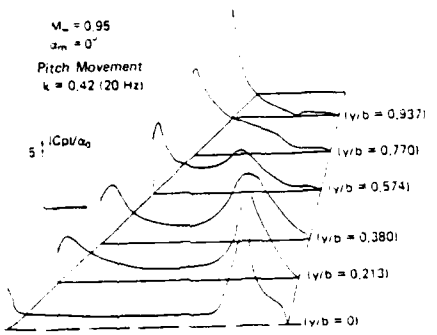

Figure 10-4. Distribution of calculated unsteady pressures at spanwise stations. Normalized amplitude/Cpl/α_0.

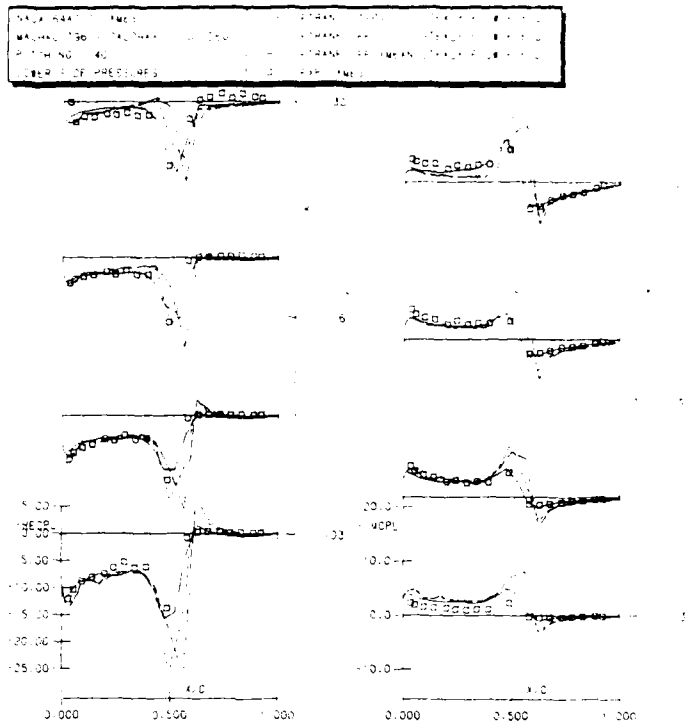

Figure 11-1. Experimental and calculated frequency-wise distributions of unsteady pressure coefficients.

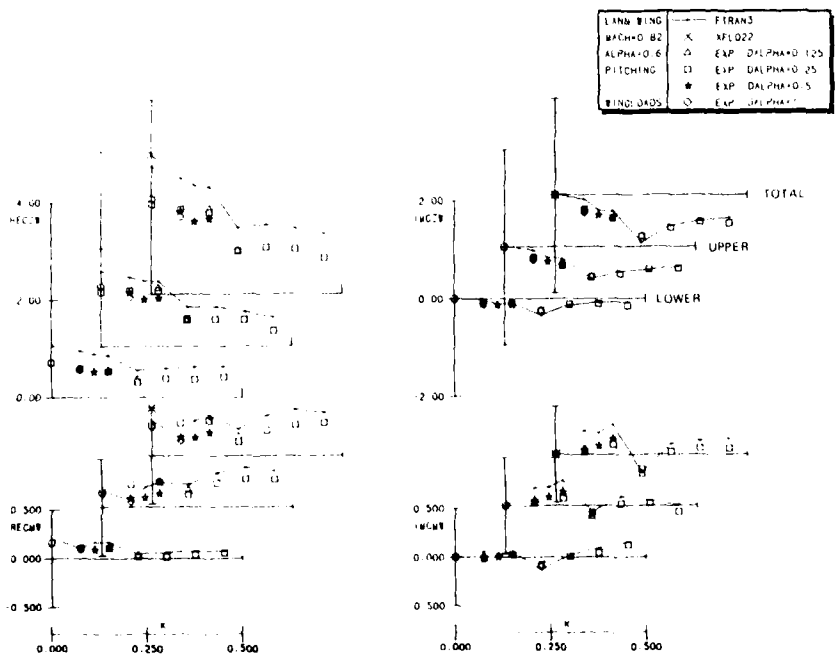

Figure 11-2. Comparison of experimental and calculated unsteady lift and moment coefficients on LANN wing.

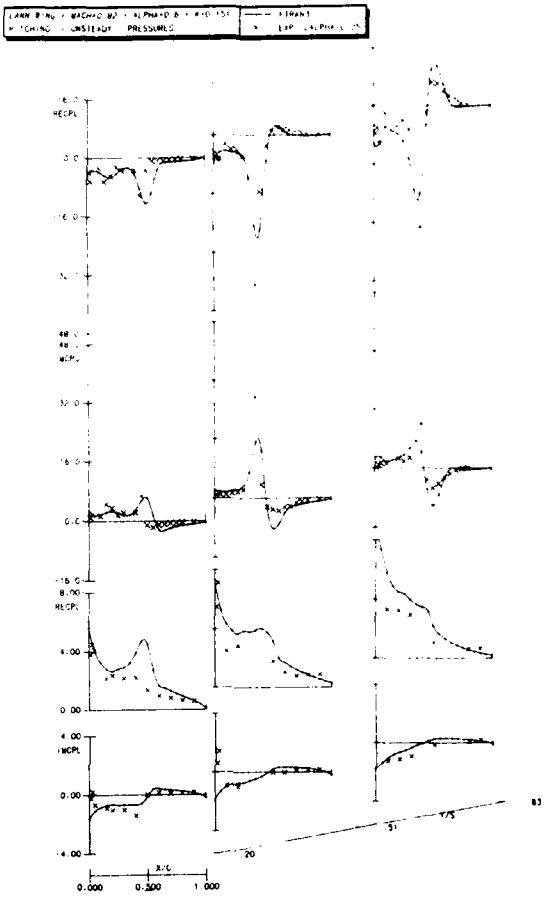

Figure 11-3. Comparison of experimental and calculated distributions of unsteady pressure coefficients at low reduced frequency.

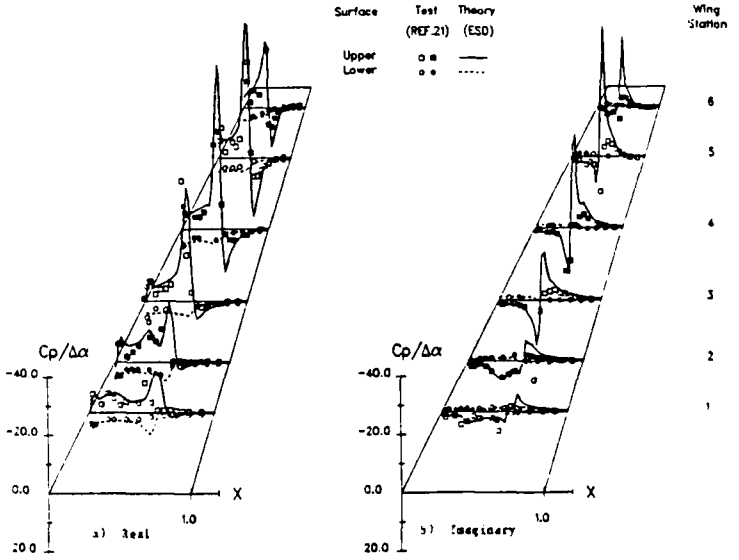

Figure 12-1. Unsteady pressures on the LANN wing, $M_\infty = 0.82$, $k = 0.076$, $\alpha_0 = 0.62$ degrees.

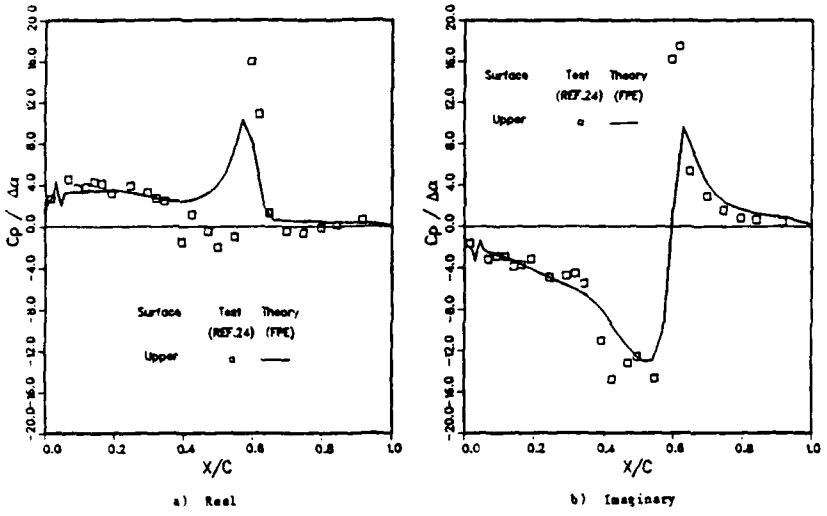

Figure 12-2. Unsteady pressures on a NLR 7301 airfoil, M_∞ = 0.751, k = 0.201, α_0 = 0.37 degrees.

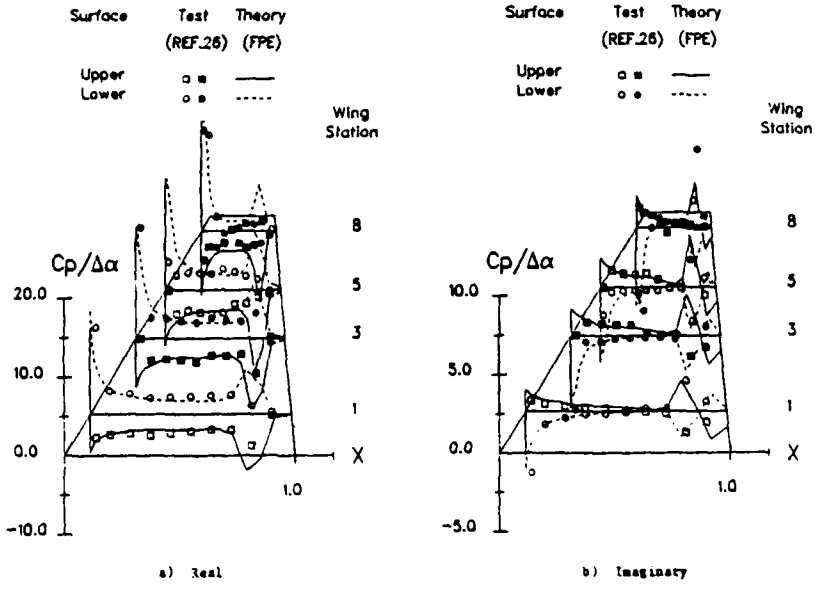

Figure 12-3. Unsteady pressures on the F-5 wing, M_∞ = 0.95, k = 0.132, α_0 = 0.0 degrees.

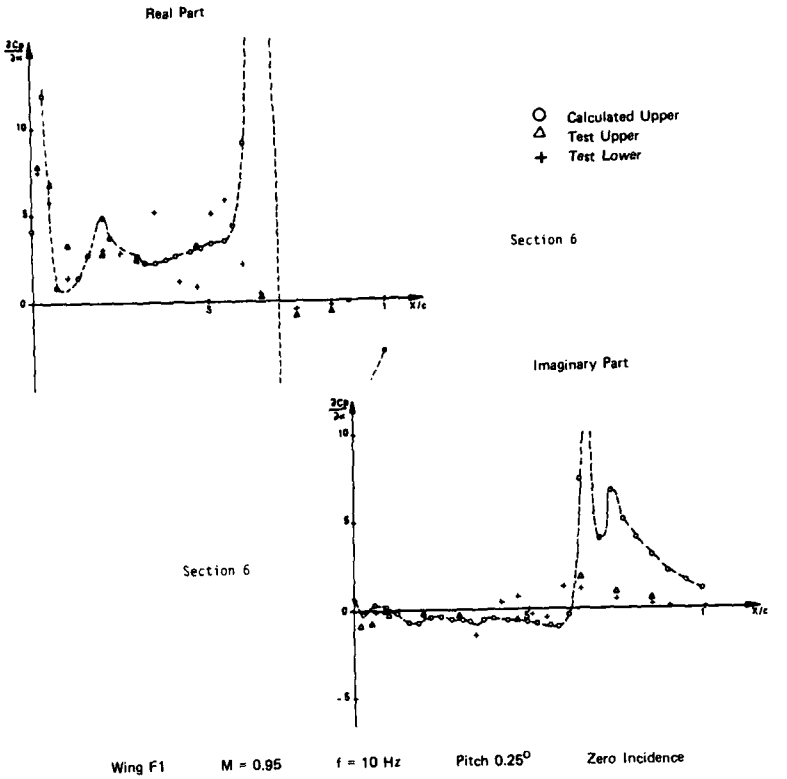

Wing F1 M = 0.95 f = 10 Hz Pitch 0.25° Zero Incidence

Figure 13-1. Comparison between theory and test of unsteady Cp.

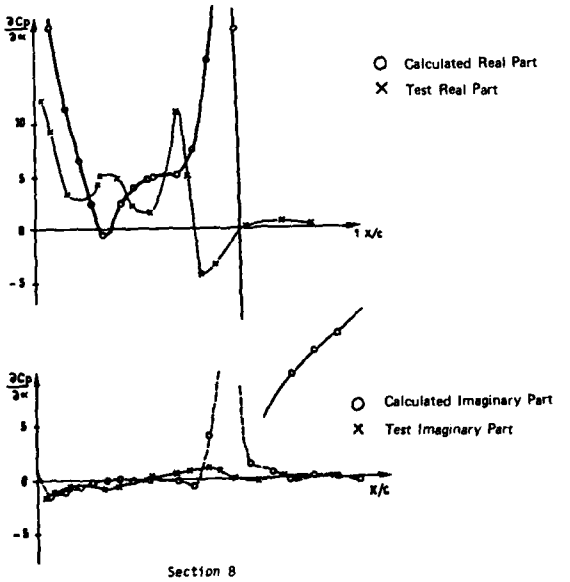

Wing F1 M = 0.95 f = 10 Hz Pitch 0.25° Zero Incidence

Figure 13-2. Comparison between theory and test of unsteady Cp.

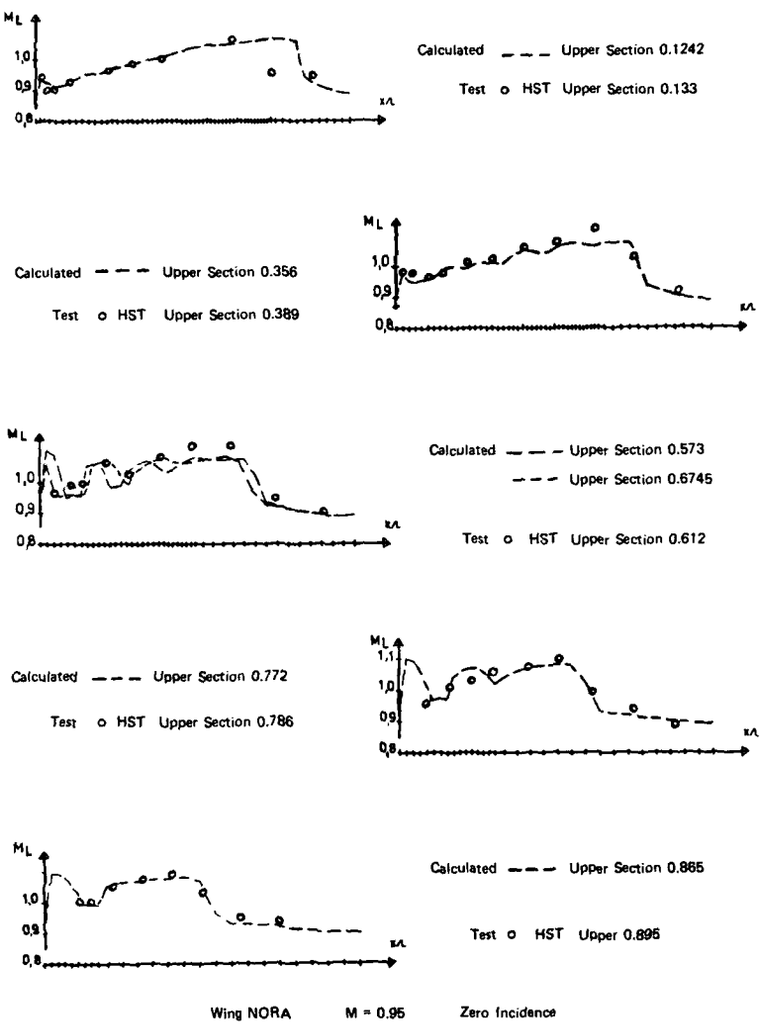

Wing NORA M = 0.95 Zero Incidence

Figure 13-3. Comparison between theory and experiment steady flow.

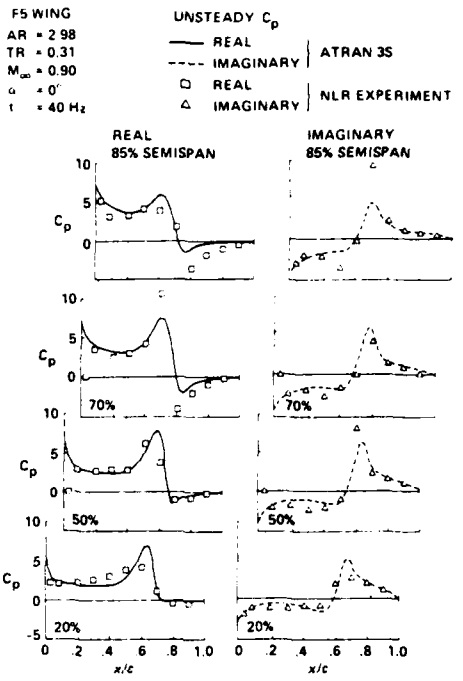

Figure 14-1. Comparison of unsteady pressures, theory and experiment: M = 0.90.

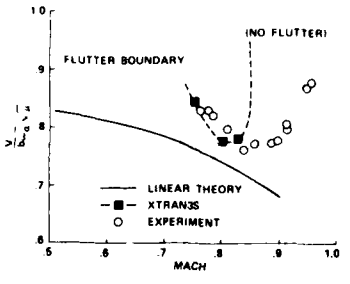

Figure 14-2. XTRAN3S flutter boundary for the Japanese transport wing.

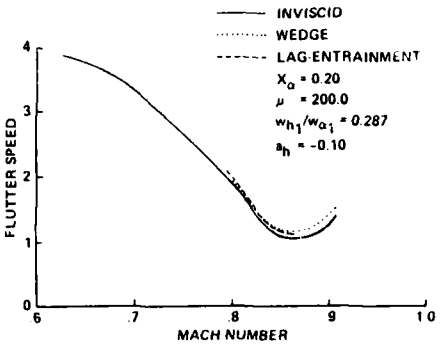

Figure 14-3. Effect of Mach number and viscosity on flutter speed of the rectangular wing.

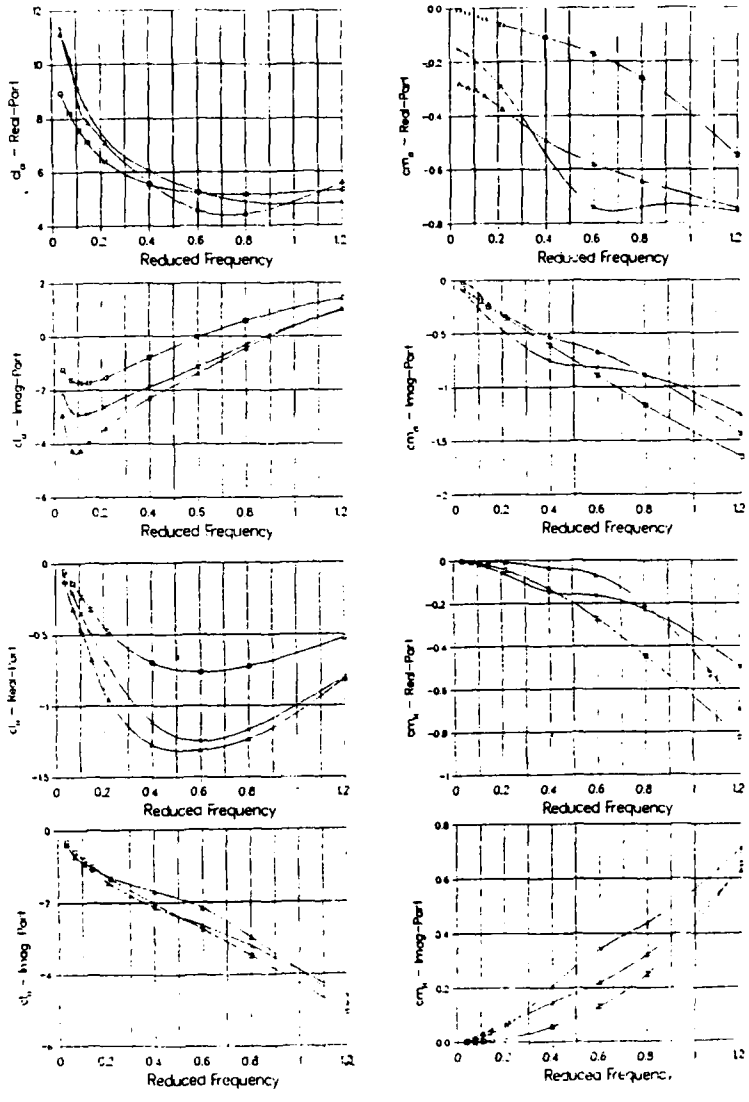

Δ TSP

× Lin. TSP

□ Doublet-Lattice

Figure 15-1. Unsteady aerodynamic coefficients: M = 0.765, α = 0.850°.

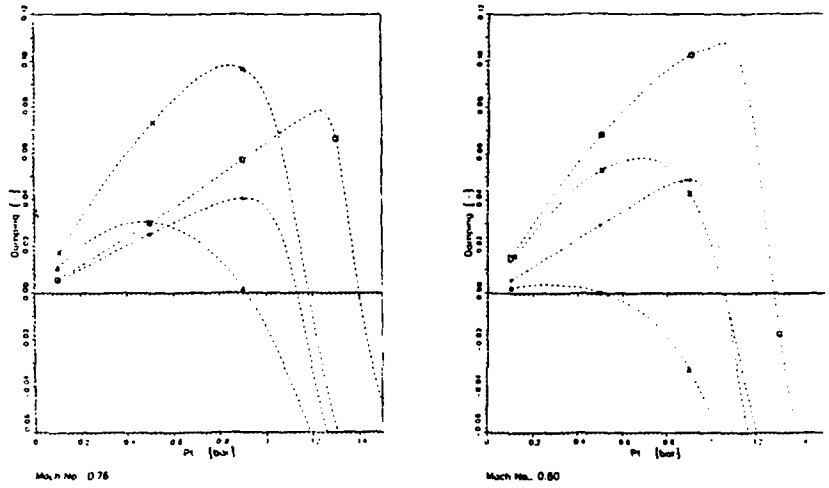

Figure 15-2. Flutter calculation results for low frequencies (f = 10 and 30 Hz).

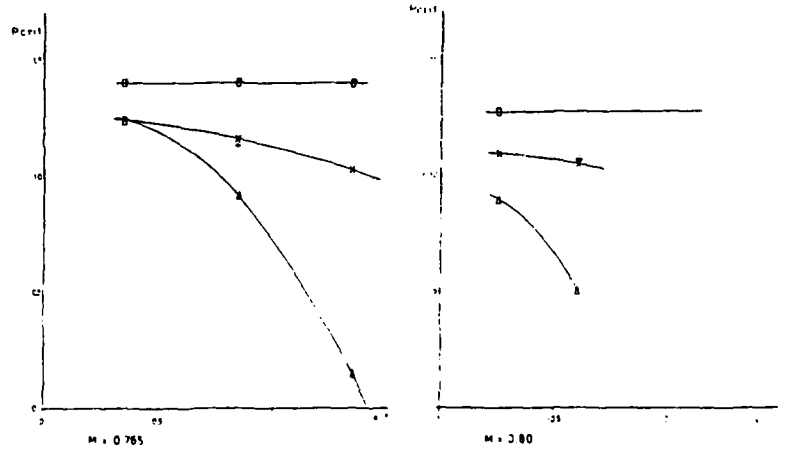

Figure 15-3. Influence of incidence on flutter for low frequencies.

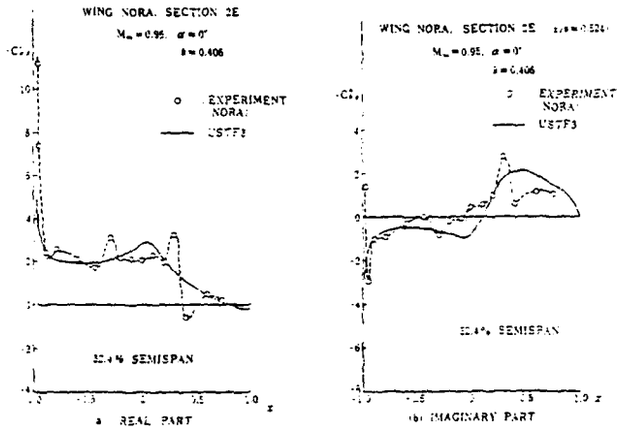

Figure 16-1. Unsteady pressure distributions (first harmonics) on upper surface of oscillating NORA Wing.

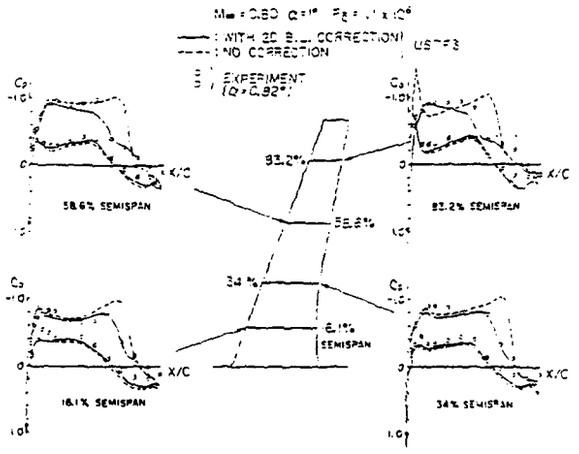

Figure 16-2. Calculated and experimental steady-state pressure distributions on high-aspect-ratio transport wing. Experimental data courtesy of JADC.

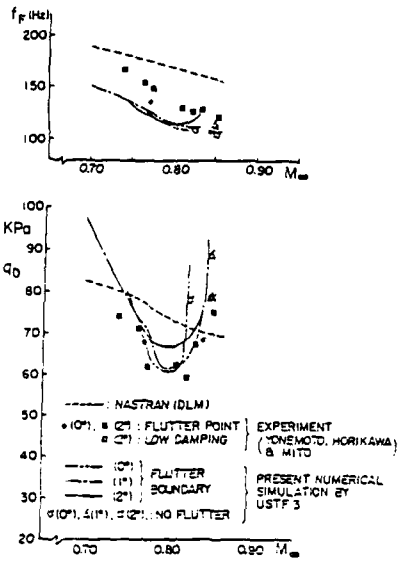

Figure 16-3. Comparison of calculated and experimental flutter boundary for high-aspect-ratio transport wing.

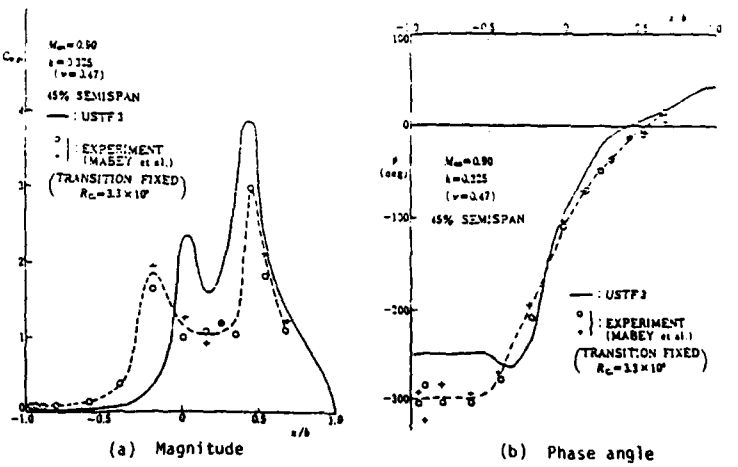

Figure 16-4. Calculated and experimental unsteady pressure distributions (first harmonics) on upper surface of RAE Swept Tapered Wing with oscillating part-span control surface.

REPORT DOCUMENTATION PAGE

1. Recipient's Reference	2. Originator's Reference	3. Further Reference	4. Security Classification of Document
	AGARD-CP-374 Addendum 1	ISBN 92-835-1501-3	UNCLASSIFIED

5. Originator Advisory Group for Aerospace Research and Development
North Atlantic Treaty Organization
7 rue Ancelle, 92200 Neuilly sur Seine, France

6. Title TRANSONIC UNSTEADY AERODYNAMICS AND ITS AEROELASTIC APPLICATIONS

7. Presented at

8. Author(s)/Editor(s)	9. Date
Various	June 1985
10. Author's/Editor's Address	**11. Pages**
Various	50

12. Distribution Statement This document is distributed in accordance with AGARD policies and regulations, which are outlined on the Outside Back Covers of all AGARD publications.

13. Keywords/Descriptors

Transonic flow
Transonic characteristics
Aerodynamics
Unsteady flow
Aeroelasticity

14. Abstract

A first section of this publication reports the papers presented to a Specialists' Meeting held by the Structures and Materials Panel at its Fall 1984 Meeting.

This addendum reviews these papers and records the Round Table Discussion.

A review of the papers at the 59th Meeting of the Structures and Materials Panel in Toulouse, France, 2—7 September 1984, together with a record of the Round Table Discussion.

AGARD Conference Proceedings No.374 Addendum 1 Advisory Group for Aerospace Research and Development, NATO TRANSONIC UNSTEADY AERODYNAMICS AND ITS AEROELASTIC APPLICATIONS Published June 1985 50 pages A first section of this publication reports the papers presented to a Specialists' Meeting held by the Structures and Materials Panel at its Fall 1984 Meeting. This addendum reviews these papers and records the Round Table Discussion. A review of the papers presented at the 59th Meeting of the P.T.O	AGARD-CP-374 Transonic flow Transonic characteristics Aerodynamics Unsteady flow Aeroelasticity	AGARD Conference Proceedings No.374 Addendum 1 Advisory Group for Aerospace Research and Development, NATO TRANSONIC UNSTEADY AERODYNAMICS AND ITS AEROELASTIC APPLICATIONS Published June 1985 50 pages A first section of this publication reports the papers presented to a Specialists' Meeting held by the Structures and Materials Panel at its Fall 1984 Meeting. This addendum reviews these papers and records the Round Table Discussion. A review of the papers presented at the 59th Meeting of the P.T.O	AGARD-CP-374 Transonic flow Transonic characteristics Aerodynamics Unsteady flow Aeroelasticity
AGARD Conference Proceedings No.374 Addendum 1 Advisory Group for Aerospace Research and Development, NATO TRANSONIC UNSTEADY AERODYNAMICS AND ITS AEROELASTIC APPLICATIONS Published June 1985 50 pages A first section of this publication reports the papers presented to a Specialists' Meeting held by the Structures and Materials Panel at its Fall 1984 Meeting. This addendum reviews these papers and records the Round Table Discussion. A review of the papers presented at the 59th Meeting of the P.T.O	AGARD-CP-374 Transonic flow Transonic characteristics Aerodynamics Unsteady flow Aeroelasticity	AGARD Conference Proceedings No.374 Addendum 1 Advisory Group for Aerospace Research and Development, NATO TRANSONIC UNSTEADY AERODYNAMICS AND ITS AEROELASTIC APPLICATIONS Published June 1985 50 pages A first section of this publication reports the papers presented to a Specialists' Meeting held by the Structures and Materials Panel at its Fall 1984 Meeting. This addendum reviews these papers and records the Round Table Discussion. A review of the papers presented at the 59th Meeting of the P.T.O	AGARD-CP-374 Transonic flow Transonic characteristics Aerodynamics Unsteady flow Aeroelasticity

Structures and Materials Panel in Toulouse, France, 2—7 September 1984, together with a record of the Round Table Discussion. ISBN 92-835-1501-3	Structures and Materials Panel in Toulouse, France, 2—7 September 1984, together with a record of the Round Table Discussion. ISBN 92-835-1501-3
Structures and Materials Panel in Toulouse, France, 2—7 September 1984, together with a record of the Round Table Discussion. ISBN 92-835-1501-3	Structures and Materials Panel in Toulouse, France, 2—7 September 1984, together with a record of the Round Table Discussion. ISBN 92-835-1501-3

AGARD

NATO ⊕ OTAN

7 RUE ANCELLE · 92200 NEUILLY-SUR-SEINE

FRANCE

Telephone 745.08.10 · Telex 610176

DISTRIBUTION OF UNCLASSIFIED AGARD PUBLICATIONS

AGARD does NOT hold stocks of AGARD publications at the above address for general distribution. Initial distribution of AGARD publications is made to AGARD Member Nations through the following National Distribution Centres. Further copies are sometimes available from these Centres, but if not may be purchased in Microfiche or Photocopy form from the Purchase Agencies listed below.

NATIONAL DISTRIBUTION CENTRES

BELGIUM
Coordonnateur AGARD – VSL
Etat-Major de la Force Aérienne
Quartier Reine Elisabeth
Rue d'Evere, 1140 Bruxelles

CANADA
Defence Scientific Information Services
Dept of National Defence
Ottawa, Ontario K1A 0K2

DENMARK
Danish Defence Research Board
Ved Idraetsparken 4
2100 Copenhagen Ø

FRANCE
O.N.E.R.A. (Direction)
29 Avenue de la Division Leclerc
92320 Châtillon

GERMANY
Fachinformationszentrum Energie,
Physik, Mathematik GmbH
Kernforschungszentrum
D-7514 Eggenstein-Leopoldshafen

GREECE
Hellenic Air Force General Staff
Research and Development Directorate
Holargos, Athens

ICELAND
Director of Aviation
c/o Flugrad
Reyjavik

ITALY
Aeronautica Militare
Ufficio del Delegato Nazionale all'AGARD
3 Piazzale Adenauer
00144 Roma/EUR

LUXEMBOURG
See Belgium

NETHERLANDS
Netherlands Delegation to AGARD
National Aerospace Laboratory, NLR
P.O. Box 126
2600 AC Delft

NORWAY
Norwegian Defence Research Establishment
Attn: Biblioteket
P.O. Box 25
N-2007 Kjeller

PORTUGAL
Portuguese National Coordinator to AGARD
Gabinete de Estudos e Programas
CLAFA
Base de Alfragide
Alfragide
2700 Amadora

TURKEY
Department of Research and Development (ARGE)
Ministry of National Defence, Ankara

UNITED KINGDOM
Defence Research Information Centre
Station Square House
St Mary Cray
Orpington, Kent BR5 3RE

UNITED STATES
National Aeronautics and Space Administration (NASA)
Langley Research Center
M/S 180
Hampton, Virginia 23665

THE UNITED STATES NATIONAL DISTRIBUTION CENTRE (NASA) DOES NOT HOLD STOCKS OF AGARD PUBLICATIONS, AND APPLICATIONS FOR COPIES SHOULD BE MADE DIRECT TO THE NATIONAL TECHNICAL INFORMATION SERVICE (NTIS) AT THE ADDRESS BELOW.

PURCHASE AGENCIES

Microfiche or Photocopy

National Technical
Information Service (NTIS)
5285 Port Royal Road
Springfield
Virginia 22161, USA

Microfiche

ESA/Information Retrieval Service
European Space Agency
10, rue Mario Nikis
75015 Paris, France

Microfiche or Photocopy

British Library Lending
Division
Boston Spa, Wetherby
West Yorkshire LS23 7BQ
England

Requests for microfiche or photocopies of AGARD documents should include the AGARD serial number, title, author or editor, and publication date. Requests to NTIS should include the NASA accession report number. Full bibliographical references and abstracts of AGARD publications are given in the following journals:

Scientific and Technical Aerospace Reports (STAR)
published by NASA Scientific and Technical
Information Branch
NASA Headquarters (NIT-40)
Washington D.C. 20546, USA

Government Reports Announcements (GRA)
published by the National Technical
Information Services, Springfield
Virginia 22161, USA

Printed by Specialised Printing Services Limited
40 Chigwell Lane, Loughton, Essex IG10 3TZ

ISBN 92-835-1501-3

END

DATE
FILMED

1-86

DTIC